

Theory of coherence in Bose-Einstein condensation phenomena in a microwave-driven interacting magnon gas

Sergio M. Rezende

Departamento de Física, Universidade Federal de Pernambuco, Recife 50670-901, PE, Brazil

(Received 29 January 2009; revised manuscript received 14 April 2009; published 11 May 2009)

Strong experimental evidences of the formation of quasiequilibrium Bose-Einstein condensation (BEC) of magnons at room temperature in a film of yttrium iron garnet (YIG) excited by microwave radiation have been recently reported. Here we present a theory for the dynamics of the magnon gas driven by a microwave field far out of equilibrium that provides rigorous support for the formation of a BEC of magnons in a YIG film magnetized in the plane. We show that if the microwave driving power exceeds a threshold value the nonlinear magnetic interactions create cooperative mechanisms for the onset of a phase transition leading to the spontaneous generation of quantum coherence and magnetic dynamic order in a macroscopic scale. The theoretical results agree with the experimental data for the intensity and the decay rate of the Brillouin light scattering from the BEC as a function of power and for the microwave emission from the uniform mode generated by the confluence of BEC magnon pairs.

DOI: [10.1103/PhysRevB.79.174411](https://doi.org/10.1103/PhysRevB.79.174411)

PACS number(s): 05.30.Jp, 03.75.Nt, 75.30.Ds

I. INTRODUCTION

In a recent series of papers Demokritov and co-workers^{1–6} reported remarkable experimental evidences of the formation of Bose-Einstein condensation (BEC) and related phenomena in a magnon gas driven by microwave radiation. Bose-Einstein condensation, a phenomenon that occurs when a macroscopic number of bosons occupies the lowest available quantum energy level,⁷ has only been unequivocally observed in a few physical systems, such as superfluids,⁷ excitons and biexcitons in semiconductors,^{8,9} atomic gases,¹⁰ and certain classes of quantum magnets.¹¹ BEC phenomena usually take place by cooling the system to very low temperatures. The room-temperature experiments reported in Refs. 1–6 ingeniously materialized earlier proposals for producing Bose-Einstein condensation of magnons^{12,13} and demonstrated powerful techniques for observing its unique properties.

The experiments were done at room temperature in epitaxial crystalline films of yttrium-iron garnet (YIG) magnetized by an applied in-plane field. In these films the combined effects of the exchange and magnetic dipolar interactions among the spins produce a dispersion relation (frequency ω_k versus wave vector k) for magnons that has a minimum ω_{k_0} at $k_0 \sim 10^5 \text{ cm}^{-1}$. In bulk samples the dispersion relation has the usual parabolic shape with a minimum at $k=0$, where the density of states vanishes. In films the energy minimum away from the Brillouin-zone center produces a peak in the density of states at ω_{k_0} , providing an important condition for the formation of the condensate.

The experiments reported in Refs. 1–6 employ a microwave magnetic field with pumping frequency $f_p=8.1 \text{ GHz}$ applied parallel to the static field to drive magnons in YIG films magnetized in the plane with the so-called parallel-pumping process.^{14,15} In some of the latest experiments reported,^{4,5} short microwave pulses (30 ns) are used to create a hot magnon gas, allowing its evolution to be observed with time-resolved Brillouin light scattering (BLS). Several important features are observed with increasing microwave

power. Initially, when the power exceeds a first threshold value, there is a large increase in the population of the parametric magnons with frequency in a narrow range around $f_p/2=4.05 \text{ GHz}$. Then the energy of these primary magnons redistributes in about 50 ns through modes with lower frequencies down to the minimum frequency $f_{\min}=\omega_{k_0}/2\pi=2.9 \text{ GHz}$ (for $H=1.0 \text{ kOe}$) as a result of magnon interactions that conserve the number of magnons. This produces a hot magnon gas that remains decoupled from the lattice for over 200 ns due to the long spin-lattice relaxation time. The BLS spectrum in this time span reflects the shape of the magnon density of states weighted by the appropriate thermal distribution exhibiting a peak at the frequency f_{\min} . Thereafter this peak decays exponentially in time in the range of several hundred ns due to the thermalization with the crystal lattice. However if the microwave power exceeds a second threshold value, much larger than the one for parallel pumping, two striking features are observed, namely, the decay rate of the BLS peak at f_{\min} doubles in value while its intensity increases by 2 orders of magnitude. The behavior of the BLS peak was attributed to a change in the magnon state from incoherent to coherent, indicating the formation of a room-temperature BEC of magnons.⁴

Coherence of photon fields has a formal quantum treatment developed by Glauber¹⁶ over 4 decades ago. Coherent magnon states, introduced in analogy with the photon states, also have a formal quantum treatment.^{17,18} In this paper we show that an interacting magnon system in a YIG film driven by microwave radiation develops spontaneous coherent states with frequencies and wave numbers in a very narrow range in phase space around k_0 , ω_{k_0} when the microwave power exceeds a critical value. As the microwave power is increased beyond threshold the number of magnons in these states approaches the number of primary magnons pumped into the system. Since the coherent states correspond to a quantum macroscopic wave function, the theory provides rigorous support for the existence of Bose-Einstein condensation of magnons in the experiments of Refs. 1–6. Note that recently it has been argued¹⁹ that the intermagnon interac-

tions in a YIG film magnetized in the plane prevent the conditions for stabilization of the BEC. Contrary to the conclusions of Ref. 19, we show that the magnon-magnon interactions play an essential role in the formation of the BEC at room temperature in a YIG film driven by microwave radiation as in the experiments of Demokritov and co-workers.¹⁻⁶

In another recent paper of the same group, Dzyapko *et al.*⁶ showed that if the applied in-plane static field has a value such that the frequency of the $k \approx 0$ magnon is $\omega_0 = 2\omega_{k_0}$, a microwave radiation signal is generated by $k \approx 0$ magnons created by pairs of BEC magnons $k_0, -k_0$ through a three-magnon confluent process. The $k \approx 0$ value is necessary for emission because the wave number of electromagnetic radiation with frequency 1.5 GHz, as in the experiments,⁶ is $k = 2\pi f/c \approx 0.3 \text{ cm}^{-1}$. In an earlier paper²⁰ we have shown that the $k \approx 0$ magnons created by the BEC are coherent magnon states, corresponding to a nearly uniform magnetization precessing with frequency ω_0 and generating a microwave signal. The microwave emission from the collective action of the spins is identified with superradiance. Here we present other aspects of the theoretical model for this phenomenon and show that the predicted radiated signal power agrees with the experimental data.⁶

The paper is organized as follows. In Sec. II we discuss the nature of the spin-wave modes in thin films based on the results of earlier work by several authors in order to establish the background for the remainder of the paper. Section III is devoted to a review of the properties of coherent magnon states. In Sec. IV we discuss the excitation of spin waves in films by the parallel-pumping technique. Section V is devoted to the proposed cooperative mechanism for the formation of the BEC of magnons. In Sec. VI we show that the states resulting from the cooperative action have quantum coherence and that the number of condensate magnons approaches the number of pumped magnons as the microwave power increases beyond the critical value for Bose-Einstein condensation. In Sec. VII we develop the theory for the microwave emission from the uniform mode generated by BEC magnon pairs. In Sec. VIII we show that the results of the model agree with experimental data for the intensity and the decay rate of the Brillouin light scattering from the BEC and for the microwave emission from the uniform mode resulting from the coalescence of a pair of BEC magnons. Section IX summarizes the main results.

II. SPIN-WAVE MODES IN THIN FILMS

Since the pioneering work of Damon and Eshbach²¹ (DE) the theory of spin waves in ferromagnetic films has been studied and reviewed by many authors.²²⁻³¹ The theory of Damon and Eshbach was developed for waves with very small wave numbers k that have energies with negligible contribution from the exchange interaction between the spins. They used a semiclassical approach for the equation of motion for the magnetization in which the magnetic dipolar field plays a dominant role. This field was obtained with the so-called magnetostatic approximation valid for wave numbers much larger than the values for the electromagnetic field

($k \sim 1 \text{ cm}^{-1}$) so DE coined the term magnetostatic waves to the resulting wave solutions. Later several authors included the exchange interaction in the equations of motion and in the boundary conditions, used various approaches and approximations to find the normal modes and introduced other names to the waves such as dipole-exchange waves. Actually they are all simply spin waves, pictured classically by the view of the spins precessing about the equilibrium direction with a phase that varies along the direction of propagation. Various results have been successfully applied to explain experimental observations in thin slabs or films of YIG and other low loss ferrite materials as well as in ultrathin films of ferromagnetic metals. In this section we present the background information on the normal spin-wave modes in a thin ferromagnetic film necessary for the discussion of the theory of the interacting spin waves. Initially we employ the DE theory extended to include exchange in order to obtain exact dispersion relations for waves in films corresponding to the nearly uniform transverse mode. Then we develop a quantum model based on the second quantization of the spin excitations involving magnon creation and annihilation operators which is the most convenient approach to treat interactions.

Consider an unbounded flat ferromagnetic film with thickness d magnetized in the plane by a static magnetic field H . We use a coordinate Cartesian system with the x and z coordinates in the plane of the film; \hat{z} along the field direction. Anisotropy is neglected since it is very small in YIG so that the magnetization \vec{M} in equilibrium lies along \hat{z} and one can write $\vec{M} = \hat{z}M_z + \hat{x}m_x + \hat{y}m_y$. The DE approach consists of solving the Landau-Lifshitz equations of motion for the small-signal time-varying components of the magnetization m_x and m_y under the action of the magnetic dipolar field they create added to the static field H .²¹ Furthermore it is assumed that m_x and m_y are described by waves with frequency ω_k and wave vector \vec{k} propagating in the film x - z plane and a standing-wave pattern in the perpendicular direction. The corresponding dipolar field \vec{h}_d can be obtained from Maxwell's equations in the magnetostatic approximation $\nabla_x \vec{h}_d = 0$, which allows expressing the field in terms of a magnetic potential ψ as $\vec{h}_d = -\nabla\psi$. The equation for ψ follows from $\nabla \cdot (\vec{h}_d + 4\pi\vec{m}) = 0$ and its solutions are subjected to the electromagnetic boundary conditions involving the internal and external fields on the two surfaces of the film. One then obtains a transcendental equation relating the frequency ω_k with the wave vector components^{21,27-29}

$$2(1 + \kappa)(-\delta)^{1/2} \cot(k_y d) + \delta(1 + \kappa)^2 - \nu^2 \sin^2 \theta_k + 1 = 0, \quad (1)$$

where θ_k is the angle between the wave vector \vec{k} in the plane and the z direction, k_y is the wave number characterizing the mode pattern in the direction normal to the film, and the other parameters are related to the frequency by

$$\kappa = \frac{\omega_H \omega_M}{\omega_H^2 - \omega_k^2}, \quad \nu = \frac{\omega_k \omega_M}{\omega_H^2 - \omega_k^2}, \quad (2)$$

and

$$\delta = \frac{1 + \kappa \sin^2 \theta_k}{1 + \kappa}, \quad (3)$$

where $\omega_H = \gamma H$, $\omega_M = \gamma 4\pi M$, and $\gamma = g\mu_B/\hbar$ is the gyromagnetic ratio (2.8 GHz/kOe for YIG). Note that the components of the wave vector \vec{k} in the plane enter in Eqs. (1)–(3) through $k_x = k \sin \theta_k$ and $k_z = k \cos \theta_k$. From the equation for the potential in the film one can see^{21,29} that the transverse wave number k_y is related to the wave number k in the plane by

$$k_y = (-\delta)^{1/2} k. \quad (4)$$

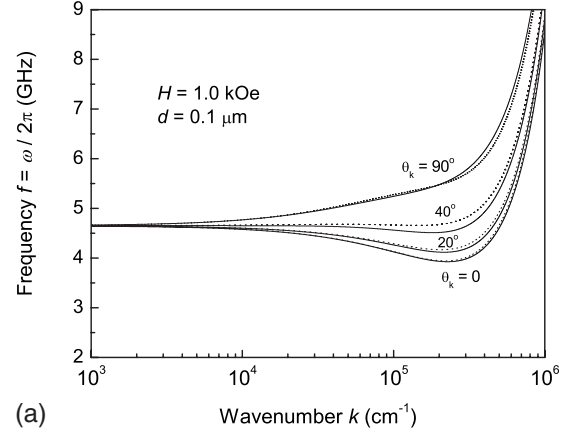
It follows that for each pair of values of k_x , k_z , or equivalently k , θ_k , Eq. (1) has several solutions for the frequency ω_k , each corresponding to a different transverse mode pattern characterized by a discrete k_y . From Eqs. (2)–(4) it is clear that k_y can be real or imaginary, depending on the range of frequency. Real values of k_y correspond to the so-called volume magnetostatic modes, for which the magnetization components have a dependence on the transverse coordinate y of the type $\cos k_y y$, $\sin k_y y$. Imaginary values of k_y correspond to the surface modes, which have an exponential dependence on y decaying away from one of the film surfaces. The surface modes have a unique property of being nonreciprocal in the sense that the wave associated with one surface propagates only in one direction but not in the opposite.^{21,22,27–29} From Eqs. (2)–(4) it can be shown^{27–29} that for each frequency there is a critical angle of propagation θ_{kc} above which δ becomes positive so that k_y is imaginary and the mode is a surface wave

$$\sin \theta_{kc} = \left(\frac{\omega_k^2 - \omega_H^2}{\omega_H \omega_M} \right)^{1/2}. \quad (5)$$

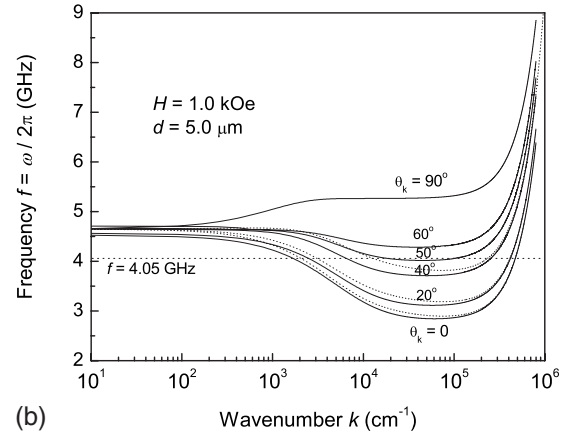
For typical numbers appropriate to the experiments of Refs. 1–6 with YIG films, $H = 1.0$ kOe, $4\pi M = 1.76$ kG, $f = \omega_k/2\pi = 4.0$ GHz, the critical angle is $\theta_{kc} = 50.26^\circ$. For the specific case of the surface wave with $\theta_k = 90^\circ$, Eq. (1) has a simple solution with an explicit dependence of the frequency on the wave vector given by²⁹

$$\omega_k^2 = \omega_H^2 + \omega_H \omega_M + \frac{1}{4} \omega_M^2 (1 - e^{-2kd}). \quad (6)$$

The introduction of the exchange interaction complicates considerably the problem of finding the spin-wave normal modes in films. First of all one can see that in films with thickness on the order of 1 μm or less, the exchange introduces a sizeable separation in the frequencies of the volume modes with different transverse patterns because $k_y \sim n_y \pi/d$ and the exchange energy varies with the square of k_y . The exact solution of the wave equations must involve the matching of mixed electromagnetic and exchange boundary conditions.^{24–26} A nearly exact expression for the frequency of the lowest lying exchange branch can be obtained by simply introducing the exchange interaction as an effective field in Eqs. (1)–(4) which is added to the applied field so that the parameter ω_H becomes



(a)



(b)

FIG. 1. Dispersion relations for spin waves propagating at various angles with the in-plane applied field $H = 1.0$ kOe in a YIG film with thicknesses (a) 0.1 μm and (b) 5 μm . The curves with full lines represent the calculation with the DE theory including exchange, Eq. (1), while the dotted lines represent the calculation with the approximate theory, Eq. (26), for $\theta_k = 0^\circ, 20^\circ$, and 40° .

$$\omega_H = \gamma(H + Dk^2), \quad (7)$$

where $D = 2JSa^2/g\mu_B$ is the exchange stiffness, J being the nearest-neighbor exchange constant, and a the lattice parameter of the film. The dispersion relations obtained by solving numerically Eqs. (1)–(4), with ω_H as in Eq. (7), are shown by the solid lines in Fig. 1 for several angles θ_k in two YIG films with thicknesses $d = 0.1$ and 5 μm using $H = 1.0$ kOe, $4\pi M = 1.76$ kG, and $D = 2 \times 10^{-9}$ Oe cm^2 . The main feature of the dispersion curves is that for propagation angles below certain values the frequency exhibits a minimum at a k value that depends on the thickness. This is a consequence of the fact that the frequency initially decreases with increasing k due to the role of the dipolar energy but then at larger values of k it changes slope due to the effect of exchange as in Eq. (7).

In the quantum approach which will be used to treat interactions we employ a Hamiltonian in the form

$$H = H_0 + H_{\text{int}} + H'(t), \quad (8)$$

where H_0 is the unperturbed Hamiltonian that describes free magnons, H_{int} represents the nonlinear magnetic interactions,

and $H'(t)$ represents the external microwave driving. The magnetic Hamiltonian can be written as $H=H_Z+H_{exc}+H_{dip}$, representing, respectively, the Zeeman, exchange and dipolar contributions. We treat the quantized excitations of the magnetic system with the approach of Holstein-Primakoff,^{32–35} which consists of three transformations that allow the spin operators to be expressed in terms of boson operators that create or destroy magnons. In the first transformation the components of the local spin operator are related to the creation and annihilation operators of spin deviation at site j , denoted, respectively, by a_j^+ and a_j , which satisfy the boson commutation rules $[a_i, a_j^+] = \delta_{ij}$ and $[a_i, a_j] = 0$. Using a coordinate system with \hat{z} along the equilibrium direction of the spins, defining $S_j^+ = S_j^x + iS_j^y$ and $S_j^- = S_j^x - iS_j^y$, where the factor i is the imaginary unit, not to be confused with the subscript denoting lattice site i , it can be shown that the relations that satisfy the commutation rules for the spin components and the boson operators are^{32–34}

$$S_j^+ = (2S)^{1/2} \left(1 - \frac{a_j^+ a_j}{2S} \right)^{1/2} a_j, \quad (9a)$$

$$S_j^- = (2S)^{1/2} a_j^+ \left(1 - \frac{a_j^+ a_j}{2S} \right)^{1/2}, \quad (9b)$$

$$S_j^z = S - a_j^+ a_j, \quad (9c)$$

where S is the spin and $a_j^+ a_j \equiv n_j$ is the operator for the number of spin deviations at site j . One of the main advantages of this approach is that the nonlinear interactions are treated analytically by expanding the square root in Eqs. (9a) and (9b) in Taylor series. We use only the first two terms of the expansion so that

$$S_j^+ \equiv (2S)^{1/2} (a_j - a_j^+ a_j / 4S) \quad \text{and} \quad (10a)$$

$$S_j^- \equiv (2S)^{1/2} (a_j^+ - a_j^+ a_j / 4S). \quad (10b)$$

In order to find the normal modes of the system we use the linear approximation, whereby only the first terms in Eqs. (9c) and (10) are kept, i.e., $S_j^+ \equiv (2S)^{1/2} a_j$, $S_j^- \equiv (2S)^{1/2} a_j^+$, and $S_j^z \equiv S$. With these transformations one can express the magnetic Hamiltonian in a quadratic form containing only lattice sums of products of two-boson operators. The second step is to introduce a transformation from the localized field operators to collective boson operators a_k^+ and a_k using the Fourier transform

$$a_j = \frac{1}{N^{1/2}} \sum_k e^{i\vec{k}\cdot\vec{r}_j} a_k, \quad (11)$$

where N is the number of spins in the system. The condition that the new collective operators satisfy the boson commutation rules $[a_k, a_{k'}^+] = \delta_{k,k'}$ and $[a_k, a_{k'}] = 0$ requires that the transformation coefficients satisfy the usual orthonormality relations. The contributions from the Zeeman and exchange energies to the Hamiltonian H_0 with quadratic form in boson operators can be shown to be^{32–35}

$$H_Z + H_{exc} = \hbar \sum_k \gamma (H + Dk^2) a_k^+ a_k. \quad (12)$$

The contribution of the dipolar energy to the Hamiltonian can be obtained with approximations valid for the nearly uniform transverse mode, which corresponds to the lowest lying exchange branch with $k_y \sim 0$. Following Refs. 30 and 31 we neglect the variation of the magnetization on the transverse coordinate and work with the averages over y ,

$$m_{x,y}(x, z; t) = m_{x,y}(\vec{r}; t) = \int_{-d/2}^{d/2} \frac{1}{d} m_{x,y}(x, z; t) dy. \quad (13)$$

The magnetic potential ψ created by the spatial variation of the small-signal transverse components of the magnetization is written in the form^{30,31}

$$\psi(x, y, z) = \frac{1}{V^{1/2}} \sum_k \psi_k(y) e^{i\vec{k}\cdot\vec{r}}, \quad (14)$$

where V is the volume of the film and \vec{k} and \vec{r} denote the wave vector and the position vector in the plane. The Fourier transform of the potential $\psi_k(y)$ can be obtained from the solution of $\nabla^2 \psi = 4\pi \nabla \cdot \vec{m}$ derived from Maxwell's equations subject to the electromagnetic boundary conditions at $y = \pm d/2$,³¹

$$\begin{aligned} \psi_k(y) = & 4\pi i [e^{-kd/2} \cosh(ky) - 1] \frac{k_x}{k^2} m_x(k) \\ & + 4\pi e^{-kd/2} \sinh(ky) \frac{1}{k} m_y(k), \end{aligned} \quad (15)$$

where the Fourier components of the magnetization appearing in Eq. (15) can be expressed in terms of the collective boson operators using Eq. (11) and the lowest-order terms in Eq. (10) in the relation $m_{x,y} = g\mu_B(N/V)S_{x,y}$,

$$m_x(k) = \hbar \gamma \left(\frac{NS}{2V} \right)^{1/2} (a_k + a_{-k}^+), \quad (16a)$$

$$m_y(k) = -i\hbar \gamma \left(\frac{NS}{2V} \right)^{1/2} (a_k - a_{-k}^+). \quad (16b)$$

The small-signal transverse components of the dipolar field can be obtained from the magnetic potential with $\vec{h}_d = -\nabla \psi$ so that the contribution of the dipolar energy to the magnetic Hamiltonian can be calculated with

$$H_{dip} = -\frac{1}{2} \int dx dy dz (m_x h_x^{dip} + m_y h_y^{dip}). \quad (17)$$

The integration in Eq. (17) can be performed without difficulty by expressing the magnetization and the dipolar field in terms of their Fourier transforms and using the orthonormality relations. One can show that

$$\begin{aligned} H_{dip} = & \hbar \gamma 2\pi M \sum_k [(1 - F_k) \sin^2 \theta_k + F_k] a_k^+ a_k \\ & + \frac{1}{2} \{ [(1 - F)_k \sin^2 \theta_k - F_k] a_k a_{-k} + \text{H.c.} \}. \end{aligned} \quad (18)$$

With Eqs. (12) and (18) one can write the total Hamiltonian for the free magnon system as

$$H_0 = \hbar \sum_k A_k a_k^+ a_k + \frac{1}{2} B_k a_k a_{-k} + \frac{1}{2} B_k a_k^+ a_{-k}^+, \quad (19)$$

where

$$A_k = \gamma [H + Dk^2 + 2\pi M(1 - F_k) \sin^2 \theta_k + 2\pi M F_k], \quad (20a)$$

$$B_k = \gamma [2\pi M(1 - F_k) \sin^2 \theta_k - 2\pi M F_k], \quad (20b)$$

$$F_k = (1 - e^{-kd})/kd. \quad (20c)$$

In order to diagonalize the quadratic Hamiltonian it is necessary to introduce new collective boson operators c_k^+ and c_k satisfying the commutation rules $[c_k, c_{k'}^+] = \delta_{kk'}$ and $[c_k, c_{k'}] = 0$, which are related to a_k^+ and a_k through the Bogoliubov transformation³²⁻³⁴

$$a_k = u_k c_k + v_k c_{-k}^+, \quad (21a)$$

$$a_k^+ = u_k c_k^+ + v_k^* c_{-k}, \quad (21b)$$

where $u_k^2 - v_k^2 = 1$ as appropriate for a unitary transformation. The coefficients of this transformation must be such that the quadratic Hamiltonian acquires the diagonal form

$$H_0 = \hbar \sum_k \omega_k c_k^+ c_k \quad (22)$$

because this leads to the Heisenberg equation of motion

$$\frac{dc_k}{dt} = \frac{1}{i\hbar} [c_k, H_0] = -i\omega_k c_k. \quad (23)$$

This equation has stationary solutions of the form $e^{-i\omega_k t}$ which assures that c_k is the operator for the normal-mode excitations of the magnetic system. Hence c_k^+ and c_k are the creation and annihilation operators for magnons. It can be shown³²⁻³⁴ that the coefficients of the transformations (21) are given,

$$u_k = \left(\frac{A_k + \omega_k}{2\omega_k} \right)^{1/2} \quad \text{and} \quad (24a)$$

$$v_k = \pm (u_k^2 - 1)^{1/2} = \pm \left(\frac{A_k - \omega_k}{2\omega_k} \right)^{1/2}, \quad (24b)$$

where the sign of v_k in Eq. (24b) is the opposite one of the parameter B_k and the frequency ω_k of the eigenmodes is

$$\omega_k = (A_k^2 - |B_k|^2)^{1/2}. \quad (25)$$

Using the expressions for the parameters in Eq. (20) we obtain from Eq. (25) an explicit equation for the dependence of the spin-wave frequency on the wave vector in the plane $\omega_k^2 = \gamma^2 [H + Dk^2 + 4\pi M(1 - F_k) \sin^2 \theta_k] [H + Dk^2 + 4\pi M F_k]$. (26)

This equation is the same as the one obtained for the lowest lying branch of the ‘‘dipole-exchange’’ modes with more rigorous treatment of the exchange interaction.²⁴⁻²⁶ It

also agrees with the results of Refs. 30 and 31 in the limit $kd \ll 1$. The dispersion curves shown by the dotted lines in Fig. 1 are obtained with Eq. (26). The agreement with the Damon-Eshbach result extended to include exchange is quite good for any angle θ_k in the YIG film with $d=0.1 \mu\text{m}$. In the case of the film with $d=5 \mu\text{m}$ the agreement is good for $\theta_k < 50^\circ$. The results in Fig. 1 show that the second quantization approach just presented describes quite well spin-wave mode in films with nearly uniform transverse pattern.

To conclude this section we express the components of the magnetization vector operators in terms of the magnon creation and annihilation operators using the relations with the spin operators and the transformations (10), (11), and (21),

$$m_x(\vec{r}) = \frac{M}{(2NS)^{1/2}} \sum_k e^{i\vec{k}\cdot\vec{r}} (u_k + v_k) (c_k + c_{-k}^*), \quad (27a)$$

$$m_y(\vec{r}) = -i \frac{M}{(2NS)^{1/2}} \sum_k e^{i\vec{k}\cdot\vec{r}} (u_k - v_k) (c_k - c_{-k}^*). \quad (27b)$$

With these equations one can calculate the expectation values of the magnetization components for any spin excitation in films expressed in terms of the magnon states.

III. COHERENT MAGNON STATES

If the nonlinear interactions are neglected, the spin-wave excitations with wave vector k and frequency ω_k described by magnon creation and annihilation operators c_k^+ and c_k form a system of independent harmonic oscillators, governed by the unperturbed Hamiltonian $H_0 = \hbar \sum \omega_k c_k^+ c_k$. The eigenstates $|n_k\rangle$ of this Hamiltonian which are also eigenstates of the number operator $n_k = c_k^+ c_k$ can be obtained by applying integral powers of the creation operator to the vacuum,

$$|n_k\rangle = [(c_k^+)^{n_k} / (n_k!)^{1/2}] |0\rangle, \quad (28)$$

where the vacuum state is defined by the condition $c_k |0\rangle = 0$. These stationary states describe systems with a precisely defined number of magnons n_k and uncertain phase. They form a complete orthonormal set which can be used as a basis for the expansion of any state of spin excitation. They are used in nearly all quantum treatments of thermodynamic properties, relaxation mechanisms, and other phenomena involving magnons. However, as can be seen from the expressions in Eq. (27), they have zero expectation value for the small-signal transverse magnetization operators m_x and m_y and thus do not have a macroscopic wave function. In order to establish a correspondence between classical and quantum spin waves one should use the concept of coherent magnon states,^{17,18} defined in analogy to the coherent photon states introduced by Glauber.¹⁶ A coherent magnon state is the eigenket of the circularly polarized magnetization operator $m^+ = m_x + im_y$. It can be written as the direct product of single-mode coherent states, defined as the eigenstates of the annihilation operator

$$c_k |\alpha_k\rangle = \alpha_k |\alpha_k\rangle, \quad (29)$$

where the eigenvalue α_k is a complex number. Although the coherent states are not eigenstates of the unperturbed Hamil-

tonian and as such do not have a well-defined number of magnons, they have nonzero expectation values for the magnetization m^+ with a well-defined phase. Here we review a few important properties of the coherent states. First we recall that they can be expanded in terms of the eigenstates of the unperturbed Hamiltonian^{16–18}

$$|\alpha_k\rangle = e^{-|\alpha_k|^2/2} \sum_{n_k} (\alpha_k)^{n_k} / (n_k!)^{1/2} |n_k\rangle. \quad (30)$$

The probability of finding n_k magnons in the coherent state $|\alpha_k\rangle$ obtained directly from Eq. (30) is given by

$$\rho_{coh}(n_k) = |\langle n_k | \alpha_k \rangle|^2 = (|\alpha_k|^{2n_k} / n_k!) e^{-|\alpha_k|^2}. \quad (31)$$

This function is a Poisson distribution¹⁶ that exhibits a peak at the expectation value of the occupation number operator $\langle n_k \rangle = |\alpha_k|^2$ in the coherent state. It can be shown that coherent states are not orthogonal to one another, but they form a complete set, so that they constitute a basis for the expansion of an arbitrary state. The distribution (31) is very different from the one prevailing in systems in thermal equilibrium, which cannot be described by pure quantum states. Instead they are described by a mixture in which one can find any number of magnons n_k with energy $\hbar\omega_k$. The average number of magnons with energy $\hbar\omega_k$ in thermal equilibrium at a temperature T is given by the Bose-Einstein distribution

$$\bar{n}_k = \frac{1}{e^{\hbar\omega_k/k_B T} - 1}, \quad (32)$$

where k_B is the Boltzmann constant. The probability of finding n_k magnons with energy $\hbar\omega_k$ in the mixture describing the thermal equilibrium with the average value (32) can be shown to be¹⁶

$$\rho_{th}(n_k) = \frac{(\bar{n}_k)^{n_k}}{(1 + \bar{n}_k)^{n_k+1}}. \quad (33)$$

Note that for large n_k Eq. (33) approaches the exponential function $\exp(-\bar{n}_k)$. To stress the difference between the coherent state and the mixture describing the thermal equilibrium we show in Fig. 2 the distributions (31) and (33) corresponding to $\langle n_k \rangle = 50$.

Another important property of a coherent state is that it can be generated by the application of a displacement operator to the vacuum^{16–18}

$$|\alpha_k\rangle = D(\alpha_k)|0\rangle, \quad (34a)$$

where

$$D(\alpha_k) = \exp(\alpha_k c_k^+ - \alpha_k^* c_k). \quad (34b)$$

In order to study the coherence properties of a magnon system, it is convenient to use the density-matrix operator ρ and its representation as a statistical mixture of coherent states,

$$\rho = \int P(\alpha_k) |\alpha_k\rangle \langle \alpha_k| d^2\alpha_k, \quad (35)$$

where $P(\alpha_k)$ is a probability density, called P representation, satisfying the normalization condition $\int P(\alpha_k) d^2\alpha_k = 1$ and $d^2\alpha_k = d(\text{Re } \alpha_k) d(\text{Im } \alpha_k)$. As shown by Glauber,¹⁶ if ρ corre-

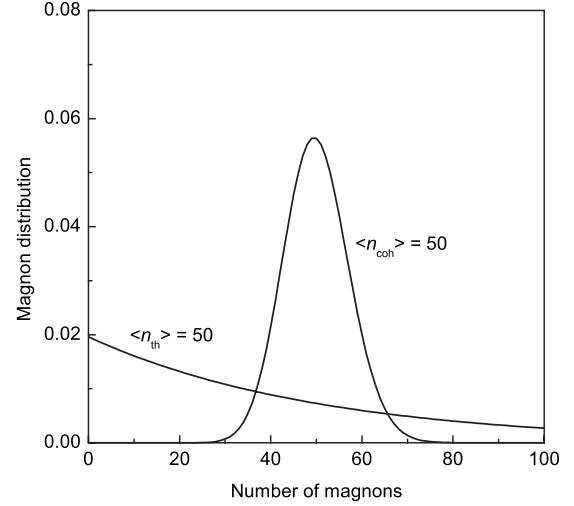


FIG. 2. Distributions of magnons in a system in thermal equilibrium and in a coherent state with $\langle n_k \rangle = 50$.

sponds to a coherent state, $P(\alpha_k)$ is a Dirac δ function. On the other hand, if ρ represents a thermal Bose-Einstein distribution, $P(\alpha_k)$ will be a Gaussian function.

To conclude this section we calculate the expectation values of the components of the magnetization operators for a single coherent state with eigenvalue $\alpha_k = |\alpha_k| \exp(i\phi_k)$. Using the definition (29) in the expressions (27) it is straightforward to show that

$$\langle m_x(\vec{r}, t) \rangle = \frac{M}{(NS/2)^{1/2}} |\alpha_k| (u_k + v_k) \cos(\vec{k} \cdot \vec{r} - \omega_k t + \phi_k), \quad (36a)$$

$$\langle m_y(\vec{r}, t) \rangle = \frac{M}{(NS/2)^{1/2}} |\alpha_k| (u_k - v_k) \sin(\vec{k} \cdot \vec{r} - \omega_k t + \phi_k). \quad (36b)$$

The transverse components of the magnetization in Eq. (36) together with $\hat{z}M_z$ correspond to the classical view of a spin wave, namely, the magnetization precesses around the equilibrium direction with a phase that varies along the direction of propagation and with an ellipticity given by

$$\frac{m_x^{\max}}{m_y^{\max}} = \left(\frac{u_k + v_k}{u_k - v_k} \right) = \frac{A_k + B_k}{\omega_k}. \quad (37)$$

Note that the elliptical precession of the transverse magnetization with frequency ω_k results in an oscillating z component with frequency $2\omega_k$. As is well known it is this fact that makes possible to excite spin waves with a microwave field parallel to the static field.

IV. MICROWAVE EXCITATION OF SPIN WAVES

Spin waves can be nonlinear excited in a magnetic material by means of several techniques employing microwave radiation, with the microwave magnetic field applied either perpendicular or parallel to the static field. The excitation is

provided by the oscillation in the coupling parameter between two or more magnon modes, so the processes are called parametric. As in other nonlinear processes, the excitation occurs when the driving field exceeds a certain threshold value which depends on the rate at which the magnon mode relaxes to the heat bath. In the parallel-pumping process the driving Hamiltonian in Eq. (8) follows from the Zeeman interaction of the microwave pumping field $\hat{z}h \cos(\omega_p t)$ with the magnetic system. One can express the Zeeman interaction in terms of the magnon operators using Eqs. (9c), (11), and (21) and keeping only terms that conserve energy and show that the driving Hamiltonian for a ferromagnetic film is given by

$$H'(t) = \frac{\hbar}{2} \sum_k h \rho_k e^{-i\omega_p t} c_k^+ c_{-k}^+ + \text{H.c.}, \quad (38a)$$

where

$$\rho_k = \gamma u_k v_k = \gamma \omega_M [(1 - F_k) \sin^2 \theta_k - F_k] / 4\omega_k \quad (38b)$$

represents the coupling of the pumping field h (frequency ω_p) with the \vec{k} , $-\vec{k}$ magnon pair with frequency ω_k equal or close to $\omega_p/2$. Note that for a thick film, a large wave vector, or a combination of both such that $kd \gg 1$ Eq. (20c) gives $F_k \ll 1$. In this case the coupling coefficient approaches the value for bulk samples $\rho_k = \gamma \omega_M \sin^2 \theta_k / 4\omega_k$. This is maximum for waves propagating perpendicularly to the field since they have the largest ellipticity and vanishes for waves with \vec{k} along the field. However in films with kd on the order of 1 or less F_k is finite and the parallel-pumping field can drive waves with any value of θ_k . This is what happens in the case of the experiments in Refs. 1–6 with $H=1.0$ kOe. As seen in Fig. 1(b) in a YIG film with $d=5$ μm magnons with frequency 4.05 GHz and $\theta_k=0$ can have two values for k , approximately $2 \times 10^3 \text{ cm}^{-1}$ and $5 \times 10^5 \text{ cm}^{-1}$. The first value corresponds to $kd \cong 1$ and $F_k \cong 0.6$ and the second to $kd \cong 250$ and $F_k \sim 0$. This means that magnons with frequency 4.05 GHz and $k \sim 2 \times 10^3 \text{ cm}^{-1}$, with $\theta_k=0$, have a finite ellipticity and can be parallel pumped. In fact, as can be seen in Fig. 1(b), for $H=1.0$ kOe only waves with θ_k in the range of from 0° to about 50° can be pumped at $f_p/2 = 4.05$ GHz. It turns out that as θ_k increases with fixed frequency the wave vector k increases so F_k decreases. In a film with thickness $d=5$ μm this approximately compensates the increase in the $\sin^2 \theta_k$ term so that the factor $u_k v_k$ which determines the parallel-pumping coupling remains about 0.2 in the whole range of θ_k from 0° to 50° .

The Heisenberg equation of motion for the operators c_k and c_k^+ with the Hamiltonian $H=H_0+H'(t)$ given by Eqs. (22) and (38) can be easily solved assuming that the pumping field is applied at $t=0$ to give the evolution of the expectation value of the number of magnons

$$\langle n_k(t) \rangle = \langle n_k(0) \rangle e^{2\lambda_k t}, \quad (39a)$$

where

$$\lambda_k = [(h\rho_k)^2 - \Delta\omega_k^2]^{1/2} - \eta_k, \quad (39b)$$

where $\langle n_k(0) \rangle$ is assumed to be the thermal number of magnons, $\Delta\omega_k = \omega_k - \omega_p/2$ is the detuning from the frequency of

maximum pumping strength, and η_k is the magnon relaxation rate which was introduced phenomenologically in the equations of motion.

Equations (39) express the well-known effect of the parallel-pumping excitation. Magnon pairs with frequency ω_k equal or close to $\omega_p/2$ and wave vectors \vec{k} , $-\vec{k}$ determined by the dispersion relation are driven parametrically and their populations grow exponentially when the field amplitude exceeds a critical value h_c , given by the condition $\lambda_k=0$ in Eq. (39b),

$$h_c = (\eta_k^2 + \Delta\omega_k^2)^{1/2} / \rho_k. \quad (40)$$

The large increase in the magnon population enhances the nonlinear interactions causing a reaction that limits its growth. Due to energy and momentum conservation the important mechanism in this process is the four-magnon interaction, which can be represented by a Hamiltonian of the form^{32–36}

$$H^{(4)} = \hbar \sum_{k,k'} \left(\frac{1}{2} S_{kk'} c_k^+ c_{-k}^+ c_{k'} c_{-k'} + T_{kk'} c_k^+ c_{k'}^+ c_k c_{k'} \right), \quad (41)$$

where the interaction coefficients are determined mainly by the dipolar and exchange energies. For the k values relevant in the experiments^{1–6} the contribution from the exchange energy is negligible compared to the dipolar.³³ The four-magnon dipolar Hamiltonian can be obtained from Eq. (17) using for \vec{m} and \vec{h}_{dip} the first and second terms of the expansions in Eq. (10), following procedures similar to those in Sec. II, and keeping only terms with two creation and two annihilation magnon operators. The result has several terms with coefficients containing the form factor F_k in Eq. (20c) and products of the parameters u_k and v_k in Eq. (24) as given in Ref. 19. It turns out that for the conditions of the experiments, $F_k \ll 1$, $u_k \sim 1$, and $v_k \ll 1$, so that the coefficients in Eq. (41) are given approximately by $S_{kk'} = 2T_{kk'} = 2\omega_M / NS$. Using the Hamiltonian (8) with Eq. (41) as the interaction term one can write the Heisenberg equations for the operators c_k and c_k^+ from which several quantities of interest can be obtained. One of them is the correlation function σ_k defined by³⁶

$$\sigma_k = \langle c_k c_{-k} \rangle = n_k e^{i\varphi_k} e^{-i2\omega_k t}, \quad (42)$$

where n_k is the magnon number operator and φ_k the phase between the states of the pair. From the equation of motion for σ_k it can be shown that for $h > h_c$, in steady state^{36–38}

$$\langle n_k \rangle_{ss} = \frac{[(h\rho_k)^2 - \eta_k^2]^{1/2} - |\Delta\omega_k|}{2V_{(4)}}, \quad (43)$$

where

$$V_{(4)} = S_{kk} + 2T_{kk} = 4\omega_M / NS. \quad (44)$$

It can also be shown that the phase φ_k varies from $-\pi/2$ to π as h increases from h_c to infinity. In the range of pumping power of the experiments^{1–6} $\varphi_k \sim -\pi/2$. By using methods of quantum statistical mechanics and the probability density defined in Eq. (35) it has been demonstrated that the magnon pairs excited by parallel pumping are in coherent magnon

states but this is so only when the four-magnon interaction is taken into account.³⁸

Equation (43) shows that magnon pairs with frequency within a certain range around $\omega_p/2$ are pumped by the microwave field when its amplitude exceeds a critical value given by

$$h_c = \frac{(\eta_k^2 + \Delta\omega_k^2)^{1/2}}{\rho_k}. \quad (45)$$

Note that the population of the parametric magnons is maximum for $\omega_k = \omega_p/2$ and for the allowed θ_k that maximizes ρ_k . The modes with $\omega_k = \omega_p/2$ are excited when the field amplitude h is larger than a critical value $h_c = \eta_k/\rho_k$. In the reported experiments the minimum h_c corresponds to a critical power p_c in the range of 100 μW to 1 mW determined by the experimental configuration and the spin-lattice relaxation rate in YIG, $\eta_{SL} \sim 2 \times 10^6 \text{ s}^{-1}$. This value is obtained from $\eta_{SL} = (2\tau_{SL})^{-1}$, where $\tau_{SL} \sim 250 \text{ ns}$ is the spin-lattice decay time of the magnon number as measured in Ref. 4. However, when very short microwave pulses are used, much higher power levels are required to reduce the rise time and to build up large magnon populations. From the numerical study of the initial time evolution of n_k for a steplike pumping and from other considerations presented in Sec. VIII, we have concluded that the relaxation rate that prevails in the dynamics is dominated by magnon-magnon scattering. This magnetic relaxation rate can be inferred from the measured decay time of the BLS peak corresponding to the primary magnons observed in Ref. 4 $\tau_m \sim 10 \text{ ns}$, so that $\eta_m \sim 25\eta_{SL} = 5 \times 10^7 \text{ s}^{-1}$. Thus one can define a critical field $h_{c1} = \eta_m/\rho_k = h_c \eta_m/\eta_{SL}$ for driving magnons out of equilibrium from the heat bath with short pulses. Using the fact that the driving microwave power p is proportional to h^2 , we can write from Eq. (43) an expression for the steady-state number of parametric magnons with frequency $\omega_k = \omega_p/2$ as a function of power

$$\langle n_k \rangle_{ss} = \frac{[(p - p_{c1})/p_{c1}]^{1/2}}{2V_{(4)}\eta_m}, \quad (46)$$

where $p_{c1} = p_c(\eta_m/\eta_{SL})^2$. Using numbers appropriate for the experiments,⁴ $p_c = 100 \mu\text{W}$, $\eta_m = 25\eta_{SL}$, $p_{c1} = 0.0625 \text{ W}$, $V_{(4)}NS = 4\omega_M = 1.24 \times 10^{11} \text{ s}^{-1}$, for a driving power $p = 4 \text{ W}$, Eq. (46) gives for the normalized number of parametric magnons $\langle n_k \rangle_{ss}/NS = 1.6 \times 10^{-3}$. The number of magnons pumped by the microwave field is actually larger than this because many modes with frequency in the vicinity of $\omega_p/2$ are also driven. From Eq. (46) one can write an approximate equation for the total number of magnons pumped into the system as

$$N_p = r_p n_H [(p - p_{c1})/p_{c1}]^{1/2}, \quad (47a)$$

where

$$n_H \equiv \eta_m/2V_{(4)} = \eta_m NS/8\omega_M \quad (47b)$$

and r_p is a factor that represents the number of pumped modes weighted by a factor relative to the number of magnons of the mode with maximum coupling.

V. MODEL FOR THE DYNAMICS OF BOSE-EINSTEIN CONDENSATION IN THE MICROWAVE-DRIVEN INTERACTING MAGNONS

In the experiments of Refs. 1–6 magnon pairs are parametrically driven by parallel pumping in a YIG film at large numbers compared to the thermal values. The population of these primary magnons with frequency equal or close to $\omega_p/2$ is quickly redistributed over a broad frequency range down to the minimum frequency $f_{\min} = \omega_{k0}/2\pi$. This redistribution is caused by four-magnon scattering events which conserve the total number of magnons so that a quasiequilibrium hot magnon gas is formed. Since the spin-lattice relaxation time in YIG is much longer than the intermagnon decay time, the hot magnon gas remains practically decoupled from the lattice for several hundred ns with an essentially constant number of magnons. In this situation the occupation number of the system is given by the Bose-Einstein distribution

$$n_{\text{BE}}(\omega, \mu, T) = \frac{1}{e^{(\hbar\omega - \mu)/k_B T} - 1}, \quad (48)$$

where μ is the associated chemical potential. As is well known⁷ in systems with constant number of particles it is Eq. (48) and not Eq. (32) that determines the distribution of the number of bosons with energy $\hbar\omega$ at a given temperature T , provided the system is in equilibrium and there is no interaction between the bosons. The experiments of Refs. 1–4 were done with 8.1 GHz microwave pumping in two types of pulsed regimes and the properties of the pumped magnon system were measured with time-resolved Brillouin light scattering. In the first one long pulses of duration 1 μs were employed to ensure that quasiequilibrium was established in the hot magnon gas while still decoupled from the lattice. This made possible the observation of the full thermal equilibrium spectra between f_{\min} and the parametric magnon frequency of 4.05 GHz as a function of the microwave pumping power. The authors of Refs. 1–4 argued that without external driving the magnons are in thermal equilibrium with the lattice and have uncertain number so that $\mu = 0$. If a microwave driving is applied and the power exceeds the threshold for parallel pumping the total number of particles in the magnon gas increases and can be expressed as

$$N_{\text{tot}} = \int D(\omega) n_{\text{BE}}(\omega, \mu, T) d\omega, \quad (49)$$

where $D(\omega)$ is the magnon density of states and the integral in Eq. (49) is carried out over the whole range of magnon frequencies. Clearly as the microwave power is raised the total number of magnons increases so that the effective temperature of the magnon gas and the chemical potential increase. Using Eq. (49) and the similar equation for the energy of the system it is possible to determine the values of μ and T for a given N_{tot} . In the experiments with long pulses^{1–3} the BLS spectra could be fitted with the spectral density function $D(\omega) n_{\text{BE}}(\omega, \mu, T)$, allowing the determination of μ and T for each power value. At a high enough power the chemical potential reaches the energy corresponding to f_{\min} resulting in an overpopulation of magnons with that frequency relative to the theoretical fit. It was then necessary to

add a singularity at f_{\min} to fit the spectrum.² This was interpreted as a signature of the Bose-Einstein condensation of magnons, namely, when the number of magnons reaches a critical value defined by the condition $\mu_c = \hbar 2\pi f_{\min}$ the gas is spontaneously divided in two parts: one with the magnons distributed according to Eq. (48) and another one with the magnons accumulated in the state of minimum energy.

The experiments with short microwave pulses (30 ns) (Refs. 4 and 5) allowed the observation of the dynamics of the redistribution of energy from the primary magnons to the modes in the broader energy range and the formation of the sole BLS peak in a narrow range in phase space centered at the wave vector k_0 along the field and frequency f_{\min} . The behaviors of the peak intensity and of the relaxation to the lattice with increasing microwave pumping power revealed that above a critical power level the magnons accumulated at the bottom of the spectrum develop a spontaneous emergence of coherence. The coherence of the BEC was further confirmed in experiments showing the microwave emission from the $k=0$ mode generated by the coalition of a pair of BEC magnons when the applied field has a value for which its frequency is $2f_{\min}$.⁶ While the thermodynamic interpretation of the experiments in Refs. 1–4 is quite satisfactory and explains qualitatively several observed features, it fails in providing quantitative results to compare to data and, most serious, it does not explain the observed spontaneous emergence of quantum coherence in the BEC of magnons. This is not surprising because a system of free noninteracting magnons cannot possibly evolve spontaneously from quantum states describing thermal magnons, represented by the distribution (33), to coherent magnons states corresponding to Eq. (31). The theory presented in this section shows that the cooperative action of the magnon gas through the four-magnon interaction can provide the mechanism for the observed spontaneous emergence of quantum coherence in the BEC. The theory relies in part on some assumptions based on the experimental observations and on some approximations to allow an analytical treatment of the problem. The ultimate justification for the assumptions and approximations is the good agreement of the theoretical results with the experimental data for the BLS intensity and for the emitted microwave signal as a function of the microwave pumping power presented in the next section.

We consider that with microwave pumping the magnon system can then be decomposed in two subsystems: one with frequency above $\omega_p/2$ in thermal equilibrium with the lattice at room temperature and another one with frequency in the range $\omega_{k_0} - \omega_p/2$ in quasiequilibrium at a higher temperature T . The second subsystem, which we call the magnon reservoir, is characterized by an occupation number given by the Bose-Einstein distribution with its own temperature and chemical potential. We also assume that after the hot magnon reservoir is formed by the redistribution of the primary magnons, the correlation between the phases of the magnon pairs lasts for a time that can be as large as $4/\eta_m$, which is about 100 ns in the experiments.^{1–6} This is a sufficient time for the four-magnon interaction to come into play for establishing a cooperative phenomenon to drive a specific k mode. The effective driving Hamiltonian for this process is obtained from Eq. (41) by taking averages of pairs of destruction op-

erators for reservoir magnons to form correlation functions as defined in Eq. (42),

$$H'(t) = \hbar \sum_{k_R} \frac{1}{2} S_{kk_R} n_{k_R} e^{i\varphi_{k_R}} e^{-i2\omega_{k_R} t} c_k^+ c_{-k}^+ + \text{H.c.} \quad (50)$$

Equation (50) has a form that resembles the Hamiltonian (38) for parallel pumping, revealing that under appropriate conditions magnon pairs can be pumped out of equilibrium in the gas. To treat Eq. (50) we note that since the number of magnons N_p pumped into the system is much larger than the number of thermal magnons in the range $\omega_{k_0} - \omega_p/2$ one can write for the magnon reservoir

$$N_p = \int D(\omega) n_{\text{BE}}(\omega, \mu, T) d\omega, \quad (51)$$

where N_p is related to the power as in Eq. (47). Of course the calculation of the population in each state of the reservoir as a function of power is a formidable task. So we use some approximations to treat the problem analytically. Consider that the population of the primary magnons is distributed among the N_R modes k_R in the magnon reservoir, so that with Eq. (47) we can write an expression for the average population of modes k_R as a function of pumping power p ,

$$n_R = r n_H [(p - p_{c1})/p_{c1}]^{1/2}, \quad (52a)$$

where

$$r = r_p/N_R. \quad (52b)$$

If all the reservoir states had the same magnon number, the sum in k_R in Eq. (50) would reproduce the density of states $D(\omega)$. Actually the number of magnons in each state k_R depends on its energy as given by Eq. (48) and can be written approximately as $n_{k_R} = f_{\text{BE}}(\omega_{k_R}) n_R$, where $f_{\text{BE}}(\omega_{k_R})$ is a function proportional to Eq. (48) with a normalization constant so that its average over the frequency range of the reservoir modes is unity,

$$f_{\text{BE}}(\omega) = n_{\text{BE}}(\omega)/C_{\text{BE}}, \quad (53a)$$

$$C_{\text{BE}} = \frac{1}{\Delta\omega_R} \int n_{\text{BE}} d\omega, \quad (53b)$$

where $\Delta\omega_R = \omega_p/2 - \omega_{k_0}$ being the frequency range of the reservoir modes. Thus the relevant quantity for determining the frequency dependence of the coefficient in the Hamiltonian (50) is the density of states weighted by the normalized Bose-Einstein distribution

$$G(\omega) = D(\omega) f_{\text{BE}}(\omega). \quad (54)$$

Note that $f_{\text{BE}}(\omega)$ and $G(\omega)$ also vary with μ and T but we omit them in the functions to simplify the notation. Figure 3 shows plots of Eq. (54) for several values of μ and the corresponding T for a 5 μm thick YIG film. The density of states was calculated numerically using the approximate dispersion relation (26) by counting the number of states with $k_x = \pm n_x 2\pi/L_x$, $k_z = \pm n_z 2\pi/L_z$ having frequencies in discrete intervals $\delta\omega = 2\pi \times 1.0$ MHz in the range $0 - \omega_p/2$. The values of μ were chosen so that their differences to $\hbar\omega_{k_0}$ are

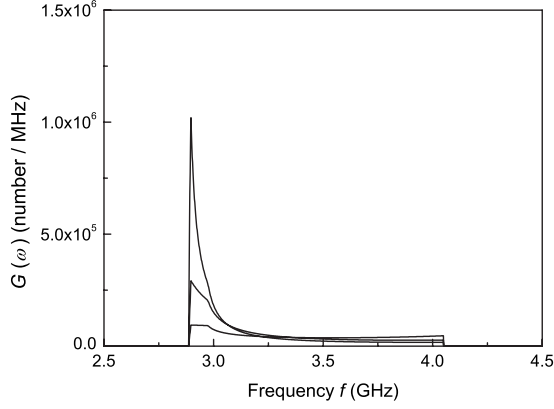


FIG. 3. $G(\omega)$ as a function of frequency for spin waves in a 5 μm thick YIG film in a field $H=1.0$ kOe with the following parameters: $\mu=0$, $T=300$ K; $\mu/h=2.718$ GHz, $T=900$ K; $\mu/h=2.868$ GHz, $T=1200$ K (h is Plank's constant; $f_{\text{min}}=2.898$ GHz).

the same as the ones used in Ref. 3 to fit the measured BLS spectra with varying microwave power. The corresponding values of T were estimated by the fits to the BLS spectra in Ref. 3. The dimensions used to calculate the density of states are $L_x=L_z=2$ mm. As expected $G(\omega)$ has a peak at the minimum frequency that becomes sharper as the chemical potential rises and approaches the minimum energy. The consequence of this is that as the microwave pumping power increases and $(\hbar\omega_{k_0}-\mu)/k_B T$ becomes very small, the peak in $G(\omega)$ dominates the coefficient in Eq. (50) revealing that it is possible to establish a cooperative action of the modes with frequency ω_{k_R} close to ω_{k_0} so as to drive magnon pairs nonlinearly as in the parallel-pumping process. Considering that the pumping is effective for frequencies ω_{k_R} in the range $\omega_{k_0} \pm \eta_m$, the sum over k_R in Eq. (50) can be replaced by $D(\omega_{k_0})\eta_m$ so that one can write an effective Hamiltonian for driving \vec{k}_0 , $-\vec{k}_0$ magnon pairs as

$$H'_{\text{eff}}(t) \cong \hbar(h\rho)_{\text{eff}} e^{-i2\omega_{k_0}t} c_{k_0}^+ c_{-k_0}^+ + \text{H.c.}, \quad (55a)$$

where

$$(h\rho)_{\text{eff}} = -iG(\omega_{k_0})\eta_m V_{(4)} n_R / 2 \quad (55b)$$

represents an effective field proportional to the average number of magnons n_R in the reservoir. Note that the factor $-i$ in Eq. (55b) arises from the phase between pairs that is approximately $-\pi/2$ in the range of power of interest. From the analysis in Sec. IV one can see that there is a critical number of reservoir modes above which they act cooperatively to pump the \vec{k}_0 , $-\vec{k}_0$ magnons parametrically. The condition $|(h\rho)_{\text{eff}}| = \eta_m$ gives the critical average number of reservoir magnons

$$n_c = 2/V_{(4)} G(\omega_{k_0}). \quad (56)$$

Since the Hamiltonian (55) has the same form as Eq. (38), the population of the k_0 mode driven by the effective field and saturated by the effect of the four-magnon interaction is calculated in the same manner as done for the direct parallel-pumping process. Thus from Eq. (43), with $\Delta\omega_k=0$, we have

$$n_{k_0} = \frac{[|(h\rho)_{\text{eff}}|^2 - \eta_m^2]^{1/2}}{2V_{(4)}}. \quad (57)$$

Using Eqs. (47b), (55b), and (56) in Eq. (57) one can write the population of the k_0 mode in terms of the average reservoir number n_R ,

$$n_{k_0} = \frac{n_H}{n_c} (n_R^2 - n_c^2)^{1/2}. \quad (58)$$

Alternatively n_{k_0} can be written in terms of the pumping power using Eqs. (52) and (56) in Eq. (58),

$$n_{k_0} = n_H [(p - p_{c2}) / (p_{c2} - p_{c1})]^{1/2}, \quad (59)$$

where n_H is given by Eq. (47b) and

$$p_{c2} = p_{c1} \{1 + 16[r\eta_m G(\omega_{k_0})]^2\} \quad (60)$$

is another threshold power level $p_{c2} \gg p_{c1}$ which will be shown to be the critical power for the formation of the BEC. Note that with Eqs. (52) and (60) the effective driving field (55b) can be expressed in terms of power as

$$(h\rho)_{\text{eff}} = -i\eta_m [(p - p_{c2}) / (p_{c2} - p_{c1})]^{1/2}. \quad (61)$$

Notice that since $G(\omega_{k_0})$ depends on μ and consequently on the power, the value of μ that enters in Eqs. (56) and (60) is the one for $p=p_{c2}$. Equations (58) and (59) are valid only for $n_R \geq n_c$ or equivalently $p \geq p_{c2}$ and they represent the first important result of this paper. For $n_R < n_c$ or $p < p_{c2}$ the population of the k_0 mode is that of thermal equilibrium with the reservoir given by

$$\bar{n}_{k_0} = n_R f_{\text{BE}}(\omega_{k_0}). \quad (62)$$

However, for $n_R \geq n_c$ or $p \geq p_{c2}$ the population of mode k_0 is pumped up out of equilibrium as a result of a spontaneous cooperative action of the reservoir modes. As it will be shown in the next section the k_0 mode with population given by Eqs. (57)–(59) above the threshold is in a coherent magnon state. This means that when the average reservoir magnon number reaches the critical value (56), the magnon gas separates in two parts: one in thermal equilibrium with the reservoir having frequencies in a wide range and one with a higher magnon number in a narrow range around the minimum frequency. This is one of the characteristic features of a Bose-Einstein condensate.

We now have the necessary elements to interpret the behavior of the magnon system with increasing microwave pumping power. First we note that in the interacting magnon gas the formation of the BEC occurs at a value of the chemical potential that is close but not equal to the minimum energy $\hbar\omega_{k_0}$. This is so because as the microwave power increases and μ approaches $\hbar\omega_{k_0}$, the average reservoir number reaches the critical value (56) corresponding to a small but finite $(\hbar\omega_{k_0}-\mu)$. The value of the chemical potential satisfying Eq. (56) can be identified as the critical value μ_c for the formation of the BEC. Using Eqs. (48), (53), (54), and (60) one can obtain the following relation between μ_c and the critical power p_{c2} :

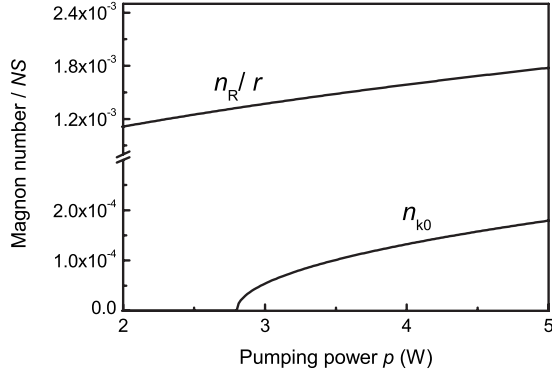


FIG. 4. Variation with microwave pumping power of the normalized reservoir average magnon number and of the k_0 magnon population.

$$\hbar\omega_{k_0} - \mu_c = \frac{r\eta_m D(\omega_{k_0})k_B T}{4C_{BE}} [(p_{c2} - p_{c1})/p_{c1}]^{1/2}, \quad (63)$$

where we have considered that $(\hbar\omega_{k_0} - \mu_c)/k_B T \ll 1$ to use the binomial expansion of the exponential function in Eq. (48). Of course Eq. (63) is not an explicit expression for the critical chemical potential in terms of p_{c2} because C_{BE} and also the effective temperature T vary with μ . Equation (63) is important to demonstrate that the difference $(\hbar\omega_{k_0} - \mu_c)$ is finite in the interacting magnon gas. As the microwave power p increases above p_{c1} , the average reservoir magnon number n_R increases continuously as given by Eq. (52). The variation of n_R with power is shown in Fig. 4. Correspondingly the chemical potential increases with power and reaches the critical value μ_c when p reaches p_{c2} , giving rise to the nonlinear driving of the k_0 mode. This process leads to a sharp increase in the magnon population at the state with minimum frequency ω_{k_0} characteristic of the condensation of bosons. For $p \geq p_{c2}$ the chemical potential locks at the value μ_c so that the dependence of $(h\rho)_{eff}$ on power is entirely contained in Eq. (61). Since the four-magnon interaction that produces the cooperative action conserves the number of magnons, as p increases further the number of magnons in the reservoir stays constant and the additional magnons originating from the primary magnons end up at the condensate state. Figure 4 also shows the variation with power of the population n_{k_0} for $p \geq p_{c2}$.

VI. QUANTUM COHERENCE OF THE BOSE-EINSTEIN MAGNON CONDENSATE

In order to study the coherence properties of the k_0 mode pumped above threshold one has to use methods of statistical mechanics appropriate for boson systems interacting with a heat bath. We follow here the same procedure used by de Araujo³⁸ to study the direct parallel-pumping process. The first step is to represent the magnon reservoir and its interactions with a specific k mode by a Hamiltonian that allows a full description of the thermal and driving processes for the interacting magnon system

$$H = H_0 + H^{(4)} + H'_{eff}(t) + H_R + H_{RS}, \quad (64)$$

where the first three terms are given respectively by Eqs. (22), (41), and (55),

$$H_R = \hbar \sum_{k_R} \omega_{k_R} c_{k_R}^+ c_{k_R} \quad (65)$$

is the Hamiltonian for the magnon reservoir, assumed to be a system with large thermal capacity and in thermal equilibrium, and

$$H_{RS} = \hbar \sum_{k, k_R} \beta_{k, k_R}^* c_{k_R}^+ c_k + \beta_{k, k_R} c_k c_{k_R}^+ \quad (66)$$

represents a linear interaction between the magnons k and the heat reservoir. Note that Eq. (66) also has its origin in the four-magnon interaction which provides the main mechanism for the intermagnon relaxation. Using the Heisenberg equation for the magnon operators for a mode k in the vicinity of k_0 with the total Hamiltonian (64) and assuming that $n_k = n_{-k}$, we obtain

$$\frac{dc_k}{dt} = -(i\omega_k + \eta_m + i2V_{(4)}n_k)c_k - i(h\rho)_{eff} e^{-i2\omega_{k_0}t} c_{-k}^+ + F_k(t), \quad (67)$$

where

$$\eta_m = \pi D(\omega_k) |\beta_{k, k_R}|^2, \quad (68a)$$

$$F_k(t) = -i \sum_{k_R} \beta_{k, k_R} c_{k_R} e^{-i\omega_{k_R}t}, \quad (68b)$$

represent, respectively, the magnetic relaxation rate expressed in terms of the interaction between magnon k and the heat reservoir and a Langevin random force with correlators of Markoffian systems type.³⁸⁻⁴⁰ Using Eq. (67) and the corresponding one for the operator c_{-k}^+ , transforming them to the representation of coherent magnon states $|\alpha_k\rangle$, and working with variables in a rotating frame $c_k|\alpha_k\rangle = \alpha_k(t)e^{-i\omega_k t}|\alpha_k\rangle$, we obtain an equation of motion for the coherent-state eigenvalue with $k \approx k_0$,

$$\frac{d\alpha_k(t)}{dt} - \frac{2V_{(4)}^2}{\eta_m} \left(\frac{|(h\rho)_{eff}|^2}{4V_{(4)}^2} - \eta_m^2 - |\alpha_k(t)|^4 \right) \alpha_k(t) = S_k(t), \quad (69a)$$

where

$$S_k(t) = F_k(t)e^{i\omega_k t} - i \frac{(h\rho)_{eff}}{\eta_m} F_{-k}^*(t)e^{-i\omega_k t}. \quad (69b)$$

Equations (69) contain all the information carried by the equations of motion for the magnon operators. It is a typical nonlinear Langevin equation which appears in Brownian motion studies and laser theory.^{39,40} It shows that the magnon modes with amplitude α_k are driven thermally by the hot magnon reservoir and also by an effective driving field. The solutions of Eq. (69) confirm the previous analysis. For negative values of the driving term $[|(h\rho)_{eff}|^2 - \eta_m^2]$ the magnon amplitudes are essentially the ones of the thermal reservoir. For positive values they grow exponentially and are limited

by the effect of the four-magnon interactions. Above the threshold condition the steady-state solution of Eq. (69) gives for the number of magnons $n_k = |\alpha_k|^2$ an expression identical to Eq. (57). The final step to obtain information about the coherence of the excited mode is to find an equation for the probability density $P(\alpha_k)$, defined in Eq. (35), that is stochastically equivalent to the Langevin equation. Using $\alpha_k = a_k \exp(i\phi_k)$ we obtain a Fokker-Plank equation in the form³⁸

$$\frac{\partial P}{\partial t'} + \frac{1}{x} \left(\frac{\partial}{\partial x} \right) [(A - x^4)x^2 P] = \frac{1}{x} \frac{\partial}{\partial x} \left(x \frac{\partial P}{\partial x} \right) + \frac{1}{x^2} \left(\frac{\partial^2 P}{\partial \phi_k^2} \right), \quad (70)$$

where

$$t' = (\bar{n}_{k0}^2 \eta_m^3 / n_H^2)^{1/3} t, \quad (71a)$$

$$x = (2/n_H^2 \bar{n}_{k0})^{1/6} a_k \quad (71b)$$

represent normalized time and magnon amplitude and the parameter A is given by

$$A = \left(\frac{2}{n_H^2 \bar{n}_{k0}} \right)^{2/3} \frac{[|(h\rho)_{eff}|^2 - \eta_m^2]^{1/2}}{2V_{(4)}} \equiv \left(\frac{2}{n_H^2 \bar{n}_{k0}} \right)^{2/3} n_{k0}^2. \quad (71c)$$

Note that A can alternatively be written in terms of the average reservoir number n_R or the power p as

$$A = \left[\frac{2n_H}{f_{BE}(\omega_{k0})n_R} \right]^{2/3} [(n_R/n_c)^2 - 1], \quad (72a)$$

$$A = \left[\frac{2}{rf_{BE}(\omega_{k0})} \right]^{2/3} \left[\frac{p_{c1}}{p - p_{c1}} \right]^{1/3} \frac{(p - p_{c2})}{(p_{c2} - p_{c1})}. \quad (72b)$$

Application of Eq. (70) to describe the full dynamics of the pulsed experiments¹⁻⁶ must consider that the factors relating t' to t and x to a_k , as well as the parameter A , are all time dependent. However, for typical numbers appropriate for the experiments, $t' \sim t \times 2 \times 10^6 \text{ s}^{-1}$, so that the dynamics of the pulsed experiments is relatively slow in the renormalized time scale. Thus in a first approximation we assume that all parameters are constant and obtain the stationary solution of Eq. (70) independent of ϕ_k in the form

$$P(x) = C \exp\left(\frac{1}{2}Ax^2 - \frac{1}{6}x^6\right), \quad (73)$$

where C is a normalization constant such that the integral of $P(x)$ in the range of x from zero to infinity is equal to unity. Note that for obtaining Eq. (73) all integration constants were set to zero to satisfy this condition. Figure 5 shows plots of $P(x)$ for four values of the parameter A : -1 , 0 , 80 , and 250 . In choosing the positive values we have considered parameters which enter in Eqs. (72a) and (72b) appropriate for the experiments:⁴ $p_c = 100 \text{ mW}$, $p_{c1} = 0.0625 \text{ W}$, and $p_{c2} = 2.8 \text{ W}$; $rf_{BE}(\omega_{k0}) \sim 7 \times 10^{-7}$ determined from Eq. (60) and using $D(\omega_{k0}) \approx 10^5 / \text{MHz}$, calculated numerically as described earlier, and $\eta_m / 2\pi = 8 \text{ MHz}$. With these numbers we

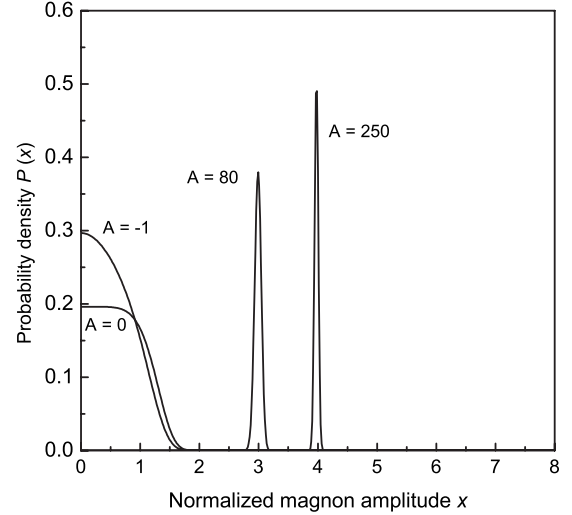


FIG. 5. Probability density characteristic of a microwave-driven interacting magnon system for several values of the parameter A : negative values correspond to $n_R < n_c$ or $p < p_{c2}$; $A=0$ corresponds to the threshold; $A=80$ and 250 correspond to $n_R/n_c = 1.008$ and 1.023 , or to $p/p_{c2} = 1.015$ and 1.047 respectively.

obtain $A=250$ for $n_R/n_c = 1.023$ or equivalently $p/p_{c2} = 1.047$.

Equation (72a) shows that for reservoir average populations below the critical number, $n_R < n_c$, the parameter A is negative. In this case the function $P(x)$ in Eq. (73) behaves as a Gaussian distribution, characteristic of systems in thermal equilibrium and described by incoherent magnon states.¹⁶ On the other hand for $n_R > n_c$ or $p > p_{c2}$, $A > 0$ and the stationary state consists of two components: a coherent one convoluted with a much smaller fluctuation with Gaussian distribution. Since the variance of $P(x)$ is proportional to A^{-1} , for $A \gg 1$ the function $P(x)$ becomes a deltalike distribution, characteristic of a coherent magnon state.¹⁶ Figure 5 shows that in the conditions of the experiments $P(x)$ becomes a deltalike function at power levels just above the critical value. Note that only in the presence of the four-magnon interaction the magnon state driven collectively by the reservoir modes is a coherent state.³⁸ Note also that $P(x)$ has a peak at $x_0 = A^{1/4}$ so that it represents a coherent state with an average number of magnons given by $x_0^2 = A^{1/2}$. From Eqs. (71b) and (71c) we see that this corresponds to a magnon number a_0^2 which is precisely the value n_{k0} given by Eqs. (58) and (59). This means that the magnon ω_{k0} driven cooperatively by the reservoir modes is a quantum coherent state. This is the second and most important result of this paper because the coherence implies a macroscopic wave function indicating that the model satisfies an essential condition for characterizing the Bose-Einstein condensation.

The calculations presented in this and the previous sections are valid for magnon pairs with frequencies and wave vectors in the vicinity of ω_{k0} and \vec{k}_0 , $-\vec{k}_0$. This fact implies that the magnons in the BEC occupy a number of states in a narrow range in phase space, which is in complete agreement with the experimental observations.⁵ This situation is called by some authors a fragmented BEC as opposed to simple BEC occurring when all particles condense in a single-

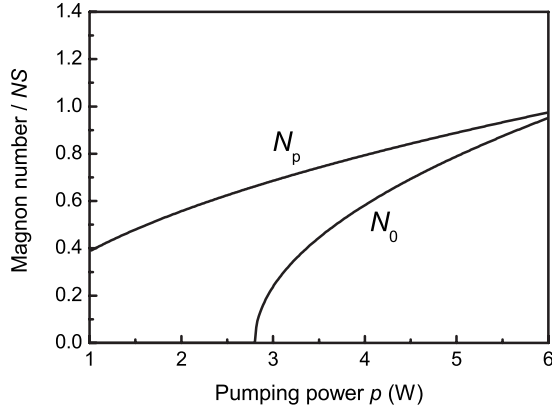


FIG. 6. Variation with microwave pumping power of the normalized number of primary pumped magnons N_p and of the BEC magnon population N_0 .

quantum state.¹⁰ The full theory of the dynamics for several modes is not a simple extension of the single-mode calculation because they are coupled by nonlinear interactions. However we can treat the system approximately assuming that the condensate consists of p_{k_0} modes governed by the single-mode equations. As will be shown in Sec. VIII the experimental data are well fit by this model with $p_{k_0}=4.4 \times 10^3$ which is a very small number compared to the number of reservoir states $N_R \sim 10^9$ calculated numerically by counting states in k space. With this approximation we consider that the number of magnons in the condensate is

$$N_0 = p_{k_0} n_{k_0}. \quad (74)$$

Figure 6 shows the variation with microwave driving power of the total number of magnons pumped into the system given by Eq. (47) and the population of the BEC magnons calculated with Eqs. (57) and (74) using parameters obtained from fit of theory to data, $p_{k_0}=4.4 \times 10^3$ and $r_p=5.0 \times 10^2$. The result of Fig. 6 represents another important feature of the Bose-Einstein condensation, namely, the number of condensate magnons approaches the total number of particles pumped into the system as the microwave power increases above the critical value. Note that these numbers represent very high magnon densities corresponding to about one spin deviation per site in the region of the condensate.

VII. THEORY OF MICROWAVE EMISSION FROM THE BEC OF MAGNONS

As observed by Dzyapko *et al.*,⁶ if the static field applied to a microwave pumped YIG film has a value such that the frequency of the $k \approx 0$ magnon is $\omega_0 = 2\omega_{k_0}$, a microwave signal is emitted with frequency ω_0 . They interpret this radiation as due to $k \approx 0$ magnons created by pairs of BEC magnons k_0 , $-k_0$ through a three-magnon confluent process. The $k \approx 0$ value is necessary for emission because the wave number of electromagnetic radiation with frequency 1.5 GHz, as in the experiments,⁶ is $k = 2\pi f/c \approx 0.3 \text{ cm}^{-1}$. Figure 7 illustrates the three-magnon confluent process in the dispersion relation for modes propagating along the field in a 5 μm thick YIG film for $H=520 \text{ Oe}$; the field value for

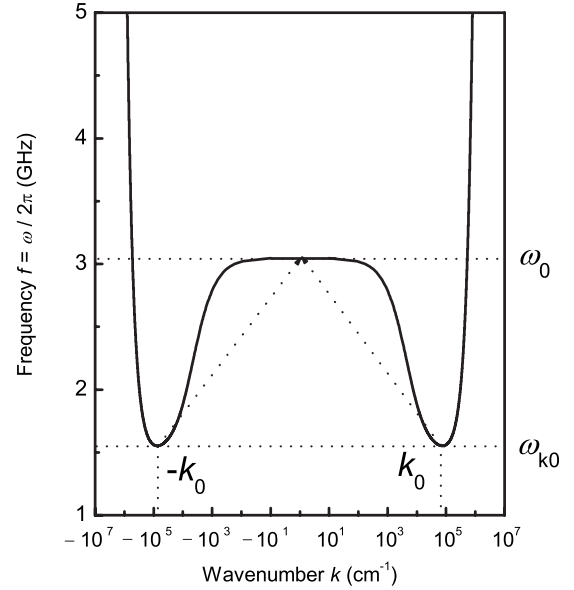


FIG. 7. Dispersion relation for magnons propagating along the field $H=520 \text{ Oe}$ applied in the plane of a YIG film with thickness 5 μm with illustration of the three-magnon coalescence process that generates a $k=0$ magnon from a pair of BEC magnons.

which $\omega_0 = 2\omega_{k_0}$. In this section we present a theoretical model for the microwave emission based on the same concepts and formalism used to explain the formation of the BEC of magnons.

The first goal of the theory is to show that the $k \approx 0$ magnons created by the BEC are coherent magnons states. This can be done using the Langevin equations for the k_0 , $-k_0$ and the $k=0$ magnons from which one obtains the probability density $P(\alpha_k)$ for the $k=0$ mode, with a calculation similar to that in Sec. VI. This has been done for the three-magnon splitting process occurring in the subsidiary resonance instability.⁴¹ Another simpler procedure consists of neglecting the thermal random forces and calculating the evolution operator for the $k=0$ state using the three-magnon interaction Hamiltonian considering that the BEC magnon pairs are in coherent states. As shown in a previous paper²⁰ this leads to the displacement operator (34) for coherent states. The end result is that above the critical microwave power p_{c2} the BEC is formed by coherent magnon pairs which coalesce to generate $k=0$ coherent magnons. These magnons correspond to a uniform magnetization precessing with frequency ω_0 that emits electromagnetic radiation with this frequency.⁴²⁻⁴⁴ To calculate the power emitted by the uniform mode as a function of the microwave pumping power we need to study the process by which this mode is driven by the BEC magnon pairs. Consider a Hamiltonian as in Eq. (8) with the magnon interactions including three- and four-magnon contributions,

$$H = H_0 + H^{(3)} + H^{(4)} + H'_{eff}(t), \quad (75)$$

where $H'_{eff}(t)$ is the effective Hamiltonian for driving \vec{k}_0 , $-\vec{k}_0$ magnon pairs given by Eqs. (55) and (61) and the Hamiltonian for the three-magnon confluence process is³²⁻³⁴

$$H^{(3)} = \hbar V_{(3)} c_0^+ c_{k_0} c_{-k_0} + \text{H.c.}, \quad (76)$$

where the vertex of the interaction for small wave vectors is dominated by the dipolar interaction between the spins S and is given approximately by $V_{(3)} = \omega_M / (2SN)^{1/2}$. To study the process by which the pairs of BEC coherent magnons \vec{k}_0 , $-\vec{k}_0$ are produced and then generate $k \sim 0$ modes, we use the Hamiltonian (75) to obtain the Heisenberg equations of motion for the magnon operators

$$\frac{dc_0}{dt} = -(i\omega_0 + \eta_0 + iV_{(4)}n_0)c_0 - iV_{(3)}c_{k_0}c_{-k_0}, \quad (77)$$

$$\begin{aligned} \frac{dc_{k_0}}{dt} = & -(i\omega_{k_0} + \eta_{k_0} + i2V_{(4)}n_{k_0})c_{k_0} \\ & - i[V_{(3)}c_0 + (h\rho)_{\text{eff}}e^{-i2\omega_{k_0}t}]c_{-k_0}^+, \end{aligned} \quad (78)$$

where the relaxation was introduced phenomenologically. We consider that all states involved are coherent magnon states as demonstrated earlier and work with the corresponding eigenvalues α_k . In addition we assume that there are p_{k_0} pair modes with wave vectors close to \vec{k}_0 , $-\vec{k}_0$ to drive the $k \sim 0$ modes and that the resonance condition is satisfied $\omega_0 = 2\omega_{k_0}$, determined by the value of the applied field H . The equations of motion for the eigenvalue α_0 and the correlation function $\sigma_{k_0} = \alpha_{k_0}\alpha_{-k_0}$ in a frame rotating with frequency ω_0 become

$$\frac{d\alpha_0}{dt} = -(\eta_0 + iV_{(4)}n_0)\alpha_0 - ip_{k_0}V_{(3)}\sigma_{k_0}, \quad (79)$$

$$\frac{d\sigma_{k_0}}{dt} = -2(\eta_{k_0} + i2V_{(4)}n_{k_0})\sigma_{k_0} - i2[V_{(3)}\alpha_0/p_{k_0} + (h\rho)_{\text{eff}}]n_{k_0}. \quad (80)$$

Note that in Eq. (80) the term representing the coupling with the $k=0$ mode is divided by the number of modes p_{k_0} assumed in the driving because σ_{k_0} represents only one pair mode k_0 . The coupling term in Eq. (80) represents a reaction of the $k=0$ mode that influences the behavior of the BEC modes. In steady state $d/dt=0$, Eq. (79) leads to

$$\alpha_0 = \frac{-ip_{k_0}V_{(3)}}{\eta_0 + iV_{(4)}n_0}\sigma_{k_0}. \quad (81)$$

This result, valid for the resonance condition $\omega_0 = 2\omega_{k_0}$, shows that the BEC magnon pairs drive the uniform mode as an effective microwave magnetic field by means of the three-magnon interaction. Note that there is no threshold condition in this process. BEC magnon pairs with any value of n_{k_0} will create $k=0$ magnons. This is in contrast to the so-called subsidiary resonance instability process in which the three-magnon splitting process occurs only if the microwave field exceeds a critical value.^{34,37,41} The presence of the term $iV_{(4)}n_0$ in the denominator due to the four-magnon interaction represents a detuning from the resonance condition due to the renormalization of the $k=0$ mode frequency. In fact, this term is responsible for the saturation in the growth of the $k=0$ mode amplitude with microwave pumping power ob-

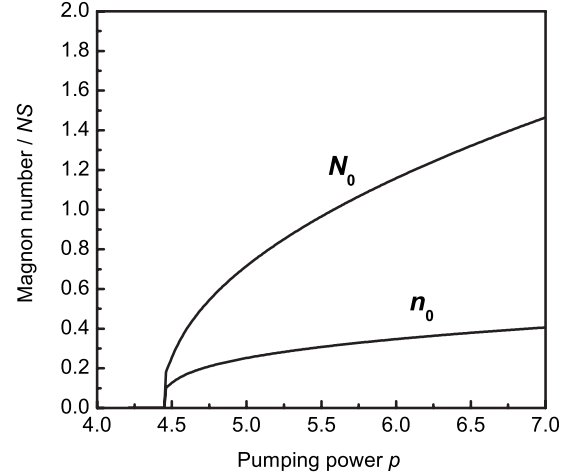


FIG. 8. Variation with microwave pumping power of the normalized steady-state magnon numbers of the uniform mode n_0 and the BEC mode $N_0 = p_{k_0}n_{k_0}$ for $p_{k_0} = 4.4 \times 10^3$.

served experimentally.⁶ In order to compare theory to data we have solved numerically the coupled Eqs. (79) and (80) with their real and imaginary parts to find the steady-state values of the magnon populations n_0 and n_{k_0} for each value of the pumping power. The calculations were done considering that the relaxation of all modes involved is dominated by the magnetic interactions, $\eta_0 = \eta_{k_0} = \eta_m$. We also use normalized dimensionless variables and parameters: $n'_k = n_k / SN$, $t' = \eta_m t$, $V'_{(3)} = V_{(3)}(SN)^{1/2} / 2\eta_m$, $V'_{(4)} = V_{(4)}(SN) / 2\eta_m$, and $(h\rho)_{\text{eff}}' = (h\rho)_{\text{eff}} / \eta_m$. With $4\pi M = 1.76$ kG and $\eta_m = 5 \times 10^7$ s⁻¹ we have $V'_{(3)} = 219.0$ and $V'_{(4)} = 1240.0$. Figure 8 shows the variation with microwave power of the normalized steady-state values of the populations of the uniform mode n_0 and the BEC magnon number N_0 given by Eq. (74). Notice that they are both nonzero only for pumping power above the threshold value which is $p_{c2} = 4.45$ W in the experiments of Ref. 6.

The total power radiated by the uniform magnetization precessing about the static field with frequency ω_0 is given by⁴⁴

$$P = \frac{2N^2\Omega^2\omega_0^4}{3c^3}(m_x^2 + m_y^2), \quad (82)$$

where N is the number of spins in the region of emission, Ω is the volume of the spin unit cell, c is the speed of light, and m_x and m_y are the small-signal components of the transverse magnetization. In Eq. (82) we have written the volume of the sample as $V = N\Omega$ to stress the dependence of the radiated power on the square of the number of spins. This characterizes superradiance, a term introduced in 1954 by Dicke⁴⁵ to designate the type of spontaneous emission of radiation from an assembly of N atoms that has as an intensity proportional to N^2 instead of N as in usual situations. This emission requires some kind of quantum coherence in the atomic states, a topic which became understood many years after Dicke's paper was published. The observation of macroscopic superradiance of microwaves in ferromagnetic resonance in YIG was achieved only in the 1970s.⁴³ The recent experiments of

Dzyapko *et al.*⁶ constitute the first observation of superradiance originating from a Bose-Einstein condensate.

VIII. COMPARISON TO EXPERIMENTAL DATA

In this section we use the model proposed for the formation of the BEC of magnons in an interacting magnon gas in a YIG film driven by microwave radiation to interpret the experimental results of Demokritov and co-workers¹⁻⁶ obtained with two very different techniques: Brillouin light scattering from magnons and microwave emission from the uniform mode driven by BEC magnon pairs. In both cases the theory developed here allows the calculation of quantities of interest as a function of microwave pumping power exhibiting very good agreement with experimental data.

A. Brillouin light scattering

In the experiments of Refs. 4 and 5 with short microwave pulse driving the coherence properties of the excited magnons states emerge clearly in the behavior of the intensity of the BLS peak at f_{\min} . As argued in Ref. 4, for incoherent scatterers the BLS intensity is proportional to their number, whereas for coherent scatterers it is proportional to the number squared. Thus to compare theory to data we express the BLS intensity in terms of the microwave power p in two regimes: $p < p_{c2}$ and $p \geq p_{c2}$. For $p < p_{c2}$ the measured intensity results from the light scattered by thermal magnons with frequencies around f_{\min} in a narrow range δf determined by the instrumental resolution. Considering that there are p_{th} states in this frequency range each with a thermal magnon population \bar{n}_{k0} given by Eqs. (52) and (62), we can write the BLS intensity for $p < p_{c2}$ as

$$I^{inc} = b \left(\frac{p_{th} \bar{n}_{k0}}{N} \right) = b r f_{BE}(\omega_{k0}) \left(\frac{p_{th} \eta_H}{N} \right) \left(\frac{p - p_{c1}}{p_{c1}} \right)^{1/2}, \quad (83)$$

where we have considered that the relevant number of scatterers is the number of magnons per spin site and b is a scale factor proportional to the magneto-optical constant involving electromagnetic, magnetic, and geometrical quantities. For $p \geq p_{c2}$ the condensate is formed by coherent magnon states with total number given by Eqs. (59) and (74) so that

$$I^{coh} = b \left(\frac{N_0}{N} \right)^2 = b \left(\frac{p_{k0} \eta_H}{N} \right)^2 \left(\frac{p - p_{c2}}{p_{c2} - p_{c1}} \right). \quad (84)$$

Figure 9 shows a fit of Eqs. (83) and (84) to data using $I^{inc} = c_1(p - p_{c1})^{1/2}$ and $I^{coh} = c_2(p - p_{c2})$, with $c_1 = 6.7$, $c_2 = 370.0$, and $p_{c2} = 2.8$ W. Using Eqs. (47b), (83), and (84) one can obtain a relation that allows the calculation of the factor $r f_{BE}(\omega_{k0})$ at the critical chemical potential from the material and fitting parameters

$$r f_{BE}(\omega_{k0}) = \frac{c_1 p_{k0}^2 \eta_m p_{c1}^{1/2}}{c_2 p_{th} 8 \omega_M p_{c2}}. \quad (85)$$

To calculate the factor in Eq. (85) one needs to have the number of states of the thermal magnons contributing to the BLS. For this we use $p_{th} = N_R \delta f / \Delta f$, where $\delta f = 50$ MHz is

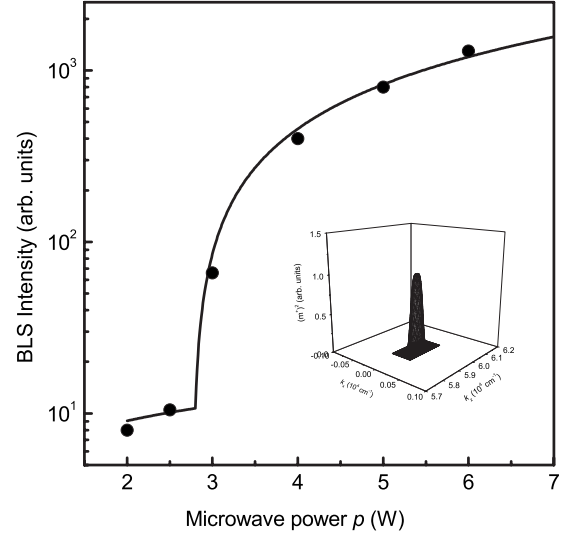


FIG. 9. Fit of the theoretical result (solid line) to the experimental data (symbols) of Demidov and co-workers (Ref. 4) for the BLS peak intensity at f_{\min} as a function of microwave pumping power. Inset shows a pictorial view of the condensate at f_{\min} represented by the distribution in k space of the square of the amplitude of the transverse magnetization.

the instrument resolution and $N_R \sim 10^9$ is the number of reservoir states calculated numerically by counting states in k space in the frequency range $\Delta f = f_p/2 - f_{\min} = 1.15$ GHz. This gives $p_{th} \sim 4 \times 10^7$. Using this number and the other parameter values we obtain $r f_{BE}(\omega_{k0}) \sim 4 \times 10^{-7}$ which is quite close to the value $r f_{BE}(\omega_{k0}) \sim 7 \times 10^{-7}$ obtained from Eq. (60) for the critical power level for BEC using $p_{c2} = 2.8$ W.

To obtain a value for $f_{BE}(\omega_{k0})$ at the critical chemical potential we use the definition (53a) and consider that the difference between the minimum energy $\hbar \omega_{k0}$ and μ_c is, in frequency units, in the range (10–20) MHz. The normalization constant C_{BE} is calculated by the integration of Eq. (53b) in the frequency range (2.9–4.05) GHz using the binomial expansion of the exponential in Eq. (48) and assuming $T = 10^3$ K. We obtain $C_{BE} = (0.8–0.9) \times 10^5$ and $f_{BE}(\omega_{k0}) \approx (10–25)$ for the range of μ_c above. With these values we have an order of magnitude estimate for $r = r_p / N_R \sim 10^{-7}$. Considering the number of reservoir states $N_R \sim 10^9$ obtained numerically, we find for the pumping factor $r_p \sim 10^2$ which is of the same order of magnitude of the value used to fit the data for the BLS decay rate.

With knowledge of the number of states in the condensate it is possible to calculate its distribution in phase space. By counting the states in $\omega - k$ space concentrated in the bottom of the magnon dispersion relation we find that $p_{k0} = 4.4 \times 10^3$ is the number of states in a frequency range of 0.07 MHz above f_{\min} . This turns out to be the frequency linewidth of the BEC of magnons, which is 2 orders of magnitude smaller than the magnon linewidth. To obtain a pictorial view of the condensate in k space we assume that the small-signal transverse magnetization m^+ is described by a Gaussian function in frequency with a peak at f_{\min} and linewidth 0.07 MHz. Using the dispersion relation we can express the

frequency in terms of the wave vector components k_x and k_z to obtain the distribution of the BEC magnetization in k space. The square of the magnetization amplitude, shown in the inset of Fig. 9, represents the BEC magnon distribution. Note that the distribution is highly asymmetric due to the anisotropy of the dispersion relation. This is consistent with the experimental results of Ref. 5 obtained with a BLS setup with wave vector resolution. However while the calculated width $\Delta k_z \sim 10^3 \text{ cm}^{-1}$ is in order of magnitude agreement with the measured value $5.6 \times 10^3 \text{ cm}^{-1}$, the calculated $\Delta k_x \sim 10^2 \text{ cm}^{-1}$ is much smaller than the measured $\Delta k_x < 3 \times 10^3 \text{ cm}^{-1}$. This discrepancy may be due to the limited k resolution of the experimental setup. From the widths of the magnon distribution in k space we can obtain the theoretical correlation lengths of the BEC of magnons, $\ell_x \sim \pi/\Delta k_x \sim 3 \times 10^{-2} \text{ cm}$ and $\ell_z \sim \pi/\Delta k_z \sim 3 \times 10^{-3} \text{ cm}$.

One of the most important results of the BLS experiments with the YIG film driven by short microwave pulses was obtained from the measurements of the time decay of the BLS peak at f_{\min} due to the relaxation of the magnon excitations to the lattice. The measurements reported⁴ reveal that as the microwave power increases above the critical value $p_{c2}=2.8 \text{ W}$, the decay rate doubles in a stepwise manner. This fact was interpreted as an indication of the emergence of coherence of the magnons in the condensed state. The argument is that if the n_k magnons causing the scattering are incoherent the intensity of the BLS peak falls exponentially in time with the same rate of the magnons. However if the magnons are coherent the BLS intensity should follow n_k^2 so that its decay rate is twice the one of the magnons. As shown in Fig. 6 the number N_0 of coherent magnons in the BEC increases with increasing microwave power above the threshold of 2.8 W and approaches the total number N_p of magnons pumped in the system at $p \sim 6 \text{ W}$. At any given power level the difference $N_p - N_0$ represents the number of incoherent magnons which, as Fig. 3 indicates, are concentrated in a narrow range of frequencies around f_{\min} thus contributing to the BLS intensity. Assuming that the decay rate η_{BLS} of the BLS peak is a linear combination of the rates for incoherent and coherent scatterers we can write

$$\eta_{\text{BLS}} = \left(\frac{N_p - N_0}{N_p} \right) 2\eta_{\text{SL}} + \frac{N_0}{N_p} 4\eta_{\text{SL}}, \quad (86)$$

where η_{SL} is the spin-lattice relaxation rate of the magnetization and $2\eta_{\text{SL}} \approx 4 \times 10^6 \text{ s}^{-1}$ is the relaxation rate of the magnon number. With Eqs. (47), (59), and (74) we can express the BLS decay rate in Eq. (86) in terms of the microwave power. The solid line in Fig. 10 represents the theoretical fit to the experimental data of Ref. 4 obtained with $p_{k0} = 4.4 \times 10^3$ and $r_p = 5.0 \times 10^2$.

B. Microwave emission from the BEC of magnons

Since the microwave signal power is a fraction of the total radiated power given by Eq. (82), we use the expression $p_s = Cn_0'$ to fit the data of Dzyapko *et al.*⁶ In Fig. 11 the symbols represent the data of Ref. 6 and the solid line represents the theoretical fit with using $C = 14.3 \text{ } \mu\text{W}$, $p_{k0} = 4.4 \times 10^3$, and $p_{c2} = 4.45 \text{ W}$. Note that the values of C and p_{k0} are slightly

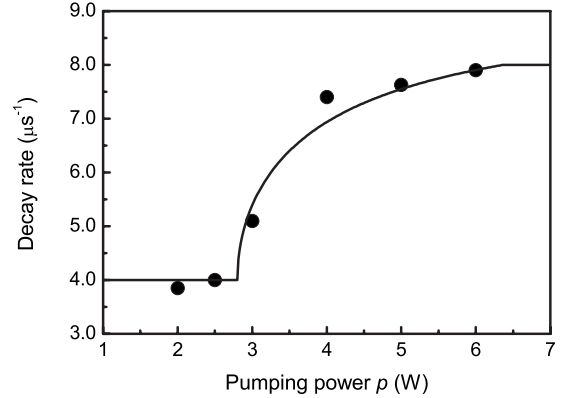


FIG. 10. Fit of the theoretical result (solid line) to the experimental data (symbols) of Demidov and co-workers (Ref. 4) for the decay rate of the BLS peak at f_{\min} as a function of microwave pumping power.

different from the ones used in Ref. 20 but the fit is equally good. It is important to check if the values of the fitting parameters bear connection to reality. To calculate the emitted microwave signal we use in Eq. (82) the expressions for the magnetization components of a coherent state (37) obtaining

$$\langle P \rangle \cong \frac{V^2 \omega_0^4 M^2}{c^3} n_0'. \quad (87)$$

Using $\omega_0 = 2\pi \times 3.0 \text{ GHz}$, $M = 300 \text{ G}$, $c = 3 \times 10^{10} \text{ cm/s}$, and an estimated emission volume $V = 1 \text{ mm} \times 0.5 \text{ mm} \times 5 \text{ } \mu\text{m} = 2.5 \times 10^{-6} \text{ cm}^3$, we obtain for the factor of n_0' in Eq. (87) approximately $400 \text{ } \mu\text{W}$. This is 2 orders of magnitude larger than the value of C obtained from the fit of theory to experiment, which is quite reasonable considering that the measured signal power is only a very small fraction of the total radiated power given by Eq. (82). It is important to note that if Eqs. (79) and (80) are solved considering $p_{k0} = 1$, the calculated n_0' is smaller than the value obtained with p_{k0}

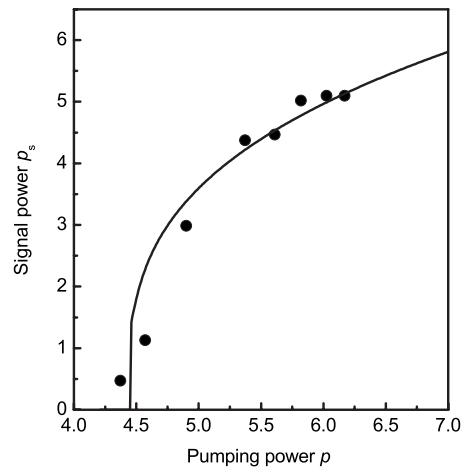


FIG. 11. Microwave emission signal power vs pumping power. Symbols represent the experimental data of Dzyapko *et al.* (Ref. 6) and solid line is the fit with theory.

$=4.4 \times 10^3$ by a factor 10^7 . This means that with $p_{k0}=1$ the total emitted power calculated with Eq. (87) would be smaller than the measured signal power by a factor 10^5 , which is completely unrealistic.

Note that this model is also consistent with the 6 MHz linewidth of the microwave emission spectrum observed in Ref. 6. This value was considered too large by the authors of Ref. 6 who expected a linewidth 1 order of magnitude smaller corresponding to the spin-lattice relaxation rate. In fact the linewidth is close to the value determined by the magnetic relaxation rate, $\eta_m/2\pi=8$ MHz, which in our theory dominates decay process. In closing this section we note that the fact that the theoretical results fit quite well several different experimental data with similar values for the various fitting parameters strongly indicates that the model is very consistent.

IX. SUMMARY AND CONCLUSIONS

We have presented a theoretical model for the dynamics of magnons in a YIG film driven by microwave radiation far out of equilibrium that provides rigorous support for the formation of Bose-Einstein condensation of magnons in the experiments of Demokritov and co-workers.¹⁻⁶ The model relies on the cooperative action of magnons with frequencies close to the minimum of the dispersion relation that is made possible by the nonlinear four-magnon interactions. The theory provides the basic requirements for the characterization of a BEC. When short microwave pulses are applied to the YIG film, magnons are pumped in large numbers and remain practically decoupled from the lattice forming a quasiequilibrium hot magnon gas. As the microwave power p is increased, the chemical potential rises and approaches the

energy of f_{\min} producing an overpopulation around that frequency. If the power p exceeds a threshold value p_{c2} the magnon density exceeds a critical value and modes in a narrow frequency range around f_{\min} are driven nonlinearly with magnetic quantum states that change from incoherent to coherent magnon states. Correspondingly, the small-signal magnetization changes from zero to $m^+ \propto (p-p_{c2})^{1/4}$. Since the magnetization represents the order parameter of the dynamic magnetic system, this characterizes a second-order phase transition with critical exponent 1/4. The spontaneous emergence of quantum coherence with the associated magnetic dynamic order in a macroscopic scale following a phase transition is one of the features of a BEC.⁴⁶ For $p > p_{c2}$ the magnon system separates in two parts: one in thermal equilibrium with the reservoir and one with N_0 magnons in coherent states having frequencies and wave vectors in a very narrow region of phase space. As the microwave power increases further N_0 approaches the total number of magnons pumped into the system characterizing unequivocally a Bose-Einstein condensation. The theoretical results fit quite well the experimental data obtained with Brillouin light scattering and with microwave emission with consistent values for the various material and fitting parameters.

ACKNOWLEDGMENTS

The author would like to thank Roberto Luzzi of UNICAMP for calling our attention to the recent challenges of BEC of magnons and Sergej Demokritov of the University of Muenster for providing important information on the experiments. The author is also very grateful to Cid B. de Araujo for many stimulating discussions and to the Ministry of Science and Technology for supporting this work.

¹S. O. Demokritov, V. E. Demidov, O. Dzyapko, G. A. Melkov, A. A. Serga, B. Hillebrands, and A. N. Slavin, *Nature (London)* **443**, 430 (2006).

²V. E. Demidov, O. Dzyapko, S. O. Demokritov, G. A. Melkov, and A. N. Slavin, *Phys. Rev. Lett.* **99**, 037205 (2007).

³O. Dzyapko, V. E. Demidov, S. O. Demokritov, G. A. Melkov, and A. N. Slavin, *New J. Phys.* **9**, 64 (2007).

⁴V. E. Demidov, O. Dzyapko, S. O. Demokritov, G. A. Melkov, and A. N. Slavin, *Phys. Rev. Lett.* **100**, 047205 (2008); S. O. Demokritov, V. E. Demidov, O. Dzyapko, G. A. Melkov, and A. N. Slavin, *New J. Phys.* **10**, 045029 (2008).

⁵V. E. Demidov, O. Dzyapko, M. Buchmeier, T. Stockhoff, G. Schmitz, G. A. Melkov, and S. O. Demokritov, *Phys. Rev. Lett.* **101**, 257201 (2008).

⁶O. Dzyapko, V. E. Demidov, S. O. Demokritov, G. A. Melkov, and V. L. Safonov, *Appl. Phys. Lett.* **92**, 162510 (2008).

⁷R. P. Feynman, *Statistical Mechanics: A Set of Lectures* (Benjamin, Reading, Massachusetts, 1972); L. D. Landau and E. M. Lifshitz, *Statistical Physics* (Pergamon, New York, 1980).

⁸See, for example, S. A. Moskalenko and D. W. Snoke, *Bose Einstein Condensation of Excitons and Biexcitons* (Cambridge University Press, Cambridge, England, 2000).

⁹J. Kasprzak *et al.*, *Nature (London)* **443**, 409 (2006).

¹⁰See, for example, *Bose Einstein Condensation in Atomic Gases*, Proceedings of the International School of Physics, "Enrico Fermi", edited by M. Inguscio, S. Stringari, and C. E. Wieman (IOS, Amsterdam, 1999); A. J. Leggett, *Rev. Mod. Phys.* **73**, 307 (2001).

¹¹See, for example, L. Yin, J. S. Xia, V. S. Zapf, N. S. Sullivan, and A. Paduan-Filho, *Phys. Rev. Lett.* **101**, 187205 (2008); G. E. Volovik, *J. Low Temp. Phys.* **153**, 266 (2008).

¹²Yu. D. Kalafati and V. L. Safonov, *Zh. Eksp. Teor. Fiz.* **95**, 2009 (1989) [*Sov. Phys. JETP* **68**, 1162 (1989)].

¹³G. A. Melkov, V. L. Safonov, A. Yu. Taranenko, and S. V. Sholom, *J. Magn. Magn. Mater.* **132**, 180 (1994).

¹⁴F. R. Morgenthaler, *J. Appl. Phys.* **31**, 95S (1960).

¹⁵E. Schlömann, J. J. Green, and V. Milano, *J. Appl. Phys.* **31**, 386S (1960).

¹⁶R. J. Glauber, *Phys. Rev.* **131**, 2766 (1963).

¹⁷S. M. Rezende and N. Zagury, *Phys. Lett.* **29A**, 47 (1969).

¹⁸N. Zagury and S. M. Rezende, *Phys. Rev. B* **4**, 201 (1971).

¹⁹I. S. Tupitsyn, P. C. E. Stamp, and A. L. Burin, *Phys. Rev. Lett.* **100**, 257202 (2008).

²⁰S. M. Rezende, *Phys. Rev. B* **79**, 060410(R) (2009).

- ²¹R. W. Damon and J. R. Eshbach, *J. Phys. Chem. Solids* **19**, 308 (1961).
- ²²M. Sparks, *Phys. Rev. B* **1**, 3831 (1970).
- ²³T. Wolfram and R. E. DeWames, *Phys. Rev. B* **4**, 3125 (1971).
- ²⁴B. A. Kalinikos, *IEEE Proc., Part H: Microwaves, Opt. Antennas* **127**, 4 (1980).
- ²⁵B. A. Kalinikos and A. N. Slavin, *J. Phys. C* **19**, 7013 (1986).
- ²⁶M. G. Cottam and A. N. Slavin, in *Linear and Nonlinear Spin Waves in Magnetic Films and Superlattices*, edited by M. G. Cottam (World Scientific, Singapore, 1994), Chap. 1.
- ²⁷D. D. Stancil, *Theory of Magnetostatic Waves* (Springer-Verlag, New York, 1993).
- ²⁸P. Kabos and V. S. Stalmachov, *Magnetostatic Waves and Their Applications* (Chapman and Hall, London, 1994).
- ²⁹M. J. Hurben and C. E. Patton, *J. Magn. Magn. Mater.* **139**, 263 (1995).
- ³⁰R. E. Arias and D. L. Mills, *Phys. Rev. B* **60**, 7395 (1999).
- ³¹P. Landeros, R. E. Arias, and D. L. Mills, *Phys. Rev. B* **77**, 214405 (2008).
- ³²M. Sparks, *Ferromagnetic Relaxation Theory* (McGraw-Hill, New York, 1964).
- ³³A. I. Akhiezer, V. G. Bar'yakhtar, and S. V. Peletminskii, *Spin Waves* (North-Holland, Amsterdam, 1968).
- ³⁴R. M. White, *Quantum Theory of Magnetism*, 3rd ed. (Springer-Verlag, Berlin, 2007).
- ³⁵S. M. Rezende, F. M. de Aguiar, and A. Azevedo, *Phys. Rev. B* **73**, 094402 (2006).
- ³⁶V. E. Zakharov, V. S. L'vov, and S. S. Starobinets, *Usp. Fiz. Nauk* **114**, 609 (1974) [*Sov. Phys. Usp.* **17**, 896 (1975)].
- ³⁷S. M. Rezende and F. M. de Aguiar, *Proc. IEEE* **78**, 893 (1990).
- ³⁸C. B. de Araujo, *Phys. Rev. B* **10**, 3961 (1974).
- ³⁹H. Haken, *Rev. Mod. Phys.* **47**, 67 (1975).
- ⁴⁰P. Meystre and M. Sargent III, *Elements of Quantum Optics* (Springer-Verlag, Berlin, 1992).
- ⁴¹C. B. de Araujo and S. M. Rezende, *Phys. Rev. B* **9**, 3074 (1974).
- ⁴²N. Bloembergen and R. V. Pound, *Phys. Rev.* **95**, 8 (1954).
- ⁴³E. Montarroyos and S. M. Rezende, *Solid State Commun.* **19**, 795 (1976).
- ⁴⁴S. Chaudhuri and F. Keffer, *J. Phys. Chem. Solids* **45**, 47 (1984).
- ⁴⁵R. H. Dicke, *Phys. Rev.* **93**, 99 (1954).
- ⁴⁶D. Snoke, *Nature (London)* **443**, 403 (2006).